*Chemical Engineering Science*, Vol. 43, No. 10, pp. 2561–2586, 1988.
Printed in Great Britain.

0009-2509/88 $3.00+0.00


# REVIEW ARTICLE NUMBER 30

# RENORMALIZATION GROUP THEORY IN SOLUTION THERMODYNAMICS

P. D. McMAHON
Department of Chemical Engineering, University of Wisconsin, Madison, WI 53706, U.S.A.

E. D. GLANDT
Department of Chemical Engineering, University of Pennsylvania, Philadelphia, PA 19104, U.S.A.

and

JAMES S. WALKER
Department of Physics, Washington State University, Pullman, WA 99164, U.S.A.

**Abstract**—Renormalization group theory is a powerful technique from condensed matter physics that has many potential applications in applied molecular thermodynamics, although it has not yet been widely used by chemical engineers. In this review the fundamental ideas of the method are described in the language of solution thermodynamics. A detailed description of a representative renormalization technique—the Migdal–Kadanoff method—is given. Applications both to simple liquid mixtures and to complex hydrogen-bonding mixtures are described.

CONTENTS



## 1. INTRODUCTION

The development of adequate thermodynamic property correlations for use in industrial process design is of vital concern to chemical engineers. Experience has shown that a combination of molecular models and statistical thermodynamics yields the best correlations for physical properties; fewer parameters are required and extrapolations tend to be more reliable than when the correlations are purely empirical. For example, Wilson has shown that a two-parameter equation derived from a simple molecular model gives a better fit to the excess free energy of binary liquid mixtures than Scatchard's five-parameter empirical curve fit (Wilson, 1964). This pragmatic blend of empiricism and statistical mechanics is known as *applied molecular thermodynamics*. Today, it is the standard approach to many problems in chemical engineering thermodynamics (Prausnitz *et al.*, 1986). Over the years, many statistical mechanical tools have been used to relate molecular models to bulk thermodynamic properties: virial expansions (Lewis and Randall, 1961), mean-field lattice theories

Table 1. Review articles on specific applications of RG theory

| Application of RG theory | Reference |
|---|---|
| Adsorption | Schick (1982) |
| Percolation and gelation | Stanley (1981) |
| | Stanley *et al.* (1982) |
| Polymers | Gennes (1979) |
| | Oono (1986) |
| | Freed (1987) |
| Chaos | Hu (1982) |
| Dynamic phenomena | Mazenko and Valls (1982) |
| Metastability | Gunton and Droz (1983) |

(Guggenheim, 1952; Abrams and Prausnitz, 1975; Lancombe and Sanchez, 1976; Kleintjens, 1983), equations of state (Redlich and Kwong, 1949; Carnahan and Starling, 1969; Peng and Robinson, 1976), perturbation theory (Smith, 1973; Henderson, 1978; Gray and Gubbins, 1984), and computer simulations (Haile, 1986; Quirke, 1986). Most recently, a new tool, *renormalization group theory*, has been added to this list. Originally developed in the study of critical point phenomena, the renormalization group (RG) has been applied to a wide variety of problems in phase equilibria, many of which are of chemical engineering interest.

Although RG theory has been the subject of several reviews in the statistical physics literature, these have been mainly addressed to physicists. In this paper, RG theory is reviewed with a view towards chemical engineering applications. The fundamental ideas underlying the RG are outlined from the point of view of solution thermodynamics, and a detailed description of a representative RG technique, the Migdal–Kadanoff (MK) method, is given. The technical details of other RG techniques and a historical perspective can be found in the following works: Wilson and Kogut (1974), Leeuwen (1975), Niemeijer and Leeuwen (1976), Ma (1976), Barber (1977), Pfeuty and Toulouse (1977), Domb (1981), Fisher (1983), Burkhardt and Leeuwen (1982), and Wilson (1975, 1979, 1983). Other reviews that focus on specific applications are listed in Table 1.

In the following section the relations from solution thermodynamics that will be needed later are reviewed, and the connection to statistical thermodynamics is outlined. In Section 3 a simple lattice model for a binary mixture is introduced; similar models yield the standard chemical engineering excess property correlations. In Sections 4–9 the RG method for calculating thermodynamic properties is described using the simple lattice mixture model as a working example. The remaining sections deal with modifications to the basis RG method, models for complex mixtures, and recent applications of the method.

## 2. THERMODYNAMIC RELATIONS

The fundamental equation for binary mixtures in the entropy representation is (Modell and Reid, 1983; Callen, 1985)

$$S = \frac{1}{T}E + \frac{P}{T}V - \frac{\mu_A}{T}N_A - \frac{\mu_A}{T}N_B$$

or, in differential form:

$$dS = \frac{1}{T}dE + \frac{P}{T}dV - \frac{\mu_A}{T}dN_A - \frac{\mu_A}{T}dN_B.$$

Here, $\mu_A$ and $\mu_B$ represent the chemical potential per molecule for species $A$ and $B$, respectively. In applying RG theory to the models to be considered later, it will prove more convenient to work in a different fundamental representation obtained by defining a Legendre transform (Callen, 1985) of the entropy as follows:

$$Y \equiv S - \frac{E}{T} + \left(\frac{\mu_A - \mu_B}{2T}\right)(N_A - N_B)$$
$$= -\left(\frac{\mu_A + \mu_B}{2T}\right)(N_A + N_B) + \frac{P}{T}V. \quad (1)$$

Known as the *semigrand thermodynamic potential*, $Y$ enjoys the property that its natural independent variables are the temperature ($T$), volume ($V$), total number of molecules ($N \equiv N_A + N_B$), and the chemical potential difference ($\Delta\mu \equiv \mu_A - \mu_B$). The differential form of the fundamental equation for this new Massieu potential is given by

$$dY = -E\,d\left(\frac{1}{T}\right) + \frac{P}{T}dV - \left(\frac{\mu_A + \mu_B}{2T}\right)dN$$
$$+ (N_A - N_B)d\left(\frac{\Delta\mu}{2T}\right). \quad (2)$$

The independent variable $\Delta\mu$ is essentially a ratio of activities or fugacities, and its thermodynamic conjugate $(N_A - N_B)$ represents the composition of the mixture, here a dependent variable. To the thermodynamic potential, $Y$, there corresponds a statistical–mechanical partition function, $\Psi$:

$$Y = k \ln \Psi \quad (3)$$

where

$$\Psi(T, \Delta\mu, V, N) \equiv \sum_{N_A=0}^{N} \sum_i \exp\left(-\frac{E_i}{kT}\right)$$
$$\times \exp\left[(N_A - N_B)\frac{\Delta\mu}{2kT}\right] \quad (4)$$

(Hill, 1956). The index $i$ in eq. (4) runs over all distinct configurations of the system, for fixed composition, while $E_i$ is the corresponding energy. Equations (2)–(4) permit the calculation of any thermodynamic property from $\Psi$ and its derivatives. For example, the composition is given by

$$(2x_A - 1) = \frac{1}{N}\left(\frac{\partial \ln \Psi}{\partial \Delta\mu / 2kT}\right)_{T,N,V}.$$

When the dependence of $E_i$ on the system's configuration has been specified, summing over all configur-

ations gives the partition function. Specifying the molecular model, i.e. $E_i$, is straightforward—except for complex substances for which the exact intermolecular potentials are rarely known (Maitland *et al.*, 1981)—but summing over all configurations is difficult, specially for complex interactions. Applied molecular thermodynamics usually simplifies both these tasks by starting from lattice models (Guggenheim, 1952).

### 3. LATTICE MODELS

Simple lattice models exhibit the qualitative behavior of fluid systems (Barker, 1963; Münster, 1969), and, although they cannot accurately predict pressure–density effects in pure fluids (Hoover *et al.*, 1964), they provide reasonable correlations for certain liquid mixture properties (Guggenheim, 1952; Abrams and Prausnitz, 1975; Lancombe and Sanchez, 1976; Panayiotou and Vera, 1980). In fact, most of the excess property equations used in chemical engineering are based on lattice models. Given the complexity of the liquid mixtures that interest chemical engineers, and the large computational effort required for such mixtures in a perturbation theory or integral equation approach, lattice mixture models will likely continue in wide use for some time.

Lattice models take a particularly simple form for mixtures of nonelectrolytes because these do not involve long-range intermolecular potentials; the important interactions generally extend for only one or two coordination shells in the fluid. Since short-range differences in the intermolecular potentials dominate the excess properties (Rowlinson and Swinton, 1982), the model need only include interactions between molecules on neighbouring lattice sites—the lattice spacing roughly corresponds to the average separation of neighboring molecules in the real mixture. Neglecting all long-range interactions greatly simplifies the calculation of $\Psi$. To compensate for the errors introduced by this approximation, the nearest-neighbor interactions can be treated as free energies or effective interactions. Their strengths are then determined empirically by correlating bulk properties. In models for simple mixtures, the interactions will only depend on the types of molecules occupying the sites. For more complex mixtures, the short-range interactions can be given an additional orientational dependence, so that effects such as hydrogen-bonding can be modeled (Barker, 1952; Tompa, 1953; Wheeler and Andersen, 1980; Walker and Vause, 1983); such models will be considered later.

Lenz introduced the simplest lattice model for nonideal liquid mixtures, although it bears the name of his student, Ising (Brush, 1967; Domb, 1974). Lenz and Ising were actually interested in modeling ferromagnetism, but it was subsequently found that the Ising model applies equally well to simple mixtures [see Hill (1956) for example]. Despite the simplicity of the model, it captures many of the essential features of nonideal mixtures, and in the following sections it will be used for illustrating the RG method. In the model, molecules are assumed to be spherically symmetric, so that the nearest-neighbor pair interaction energies depend only on the molecular identities—there are no orientational effects. Furthermore, size effects are not considered, so that each molecule occupies only one lattice site. Thus, the energy of a particular lattice configuration is given by

$$E_i = N_{AA}\varepsilon_{AA} + N_{BB}\varepsilon_{BB} + N_{AB}\varepsilon_{AB} \tag{5}$$

where $N_{ij}$ is the number of nearest-neighbor pairs of type $ij$ and $\varepsilon_{ij}$ is the corresponding interaction energy. The geometric structure of the lattice imposes constraints on the $N_{ij}$. If $z$ is the lattice coordination number ($z = 6$ for a cubic lattice), then

$$zN_A = 2N_{AA} + N_{AB} \tag{6}$$

$$zN_B = 2N_{BB} + N_{AB}. \tag{7}$$

With these *lattice relationships*, eq. (4) becomes

$$\Psi = \sum_{N_A,i} \exp\left\{-N\left[\frac{z(\varepsilon_{AA}+\varepsilon_{BB})}{4kT}\right]\right\} \times \exp\left[-N_{AB}\left(\frac{2\varepsilon_{AB}-\varepsilon_{AA}-\varepsilon_{BB}}{2kT}\right)\right] \times \exp\left\{+(N_A-N_B)\left[\frac{2\Delta\mu - z(\varepsilon_{AA}-\varepsilon_{BB})}{4kT}\right]\right\}. \tag{8}$$

Notice that the first term, which depends on $N$, is independent of the composition and configuration. Thus, it can be moved outside the summation. The two remaining terms, in $N_{AB}$ and $(N_A - N_B)$, respectively, are the contributions of the nearest-neighbor bonds and of the individual sites. (In RG theory, the term *bond* refers to any nearest-neighbor lattice pair interaction; it does not imply a chemical bond.) It will be convenient to define a dimensionless exchange energy, $\omega$;

$$\omega \equiv (2\varepsilon_{AB} - \varepsilon_{AA} - \varepsilon_{BB})/2kT \tag{9}$$

and a dimensionless chemical potential field, $\Delta\tilde{\mu}$:

$$\Delta\tilde{\mu} \equiv [2\Delta\mu - z(\varepsilon_{AA} - \varepsilon_{BB})]/4kT.$$

With these definitions, $\Psi$ can be reexpressed as the product of two terms

$$\Psi(T, \Delta\mu; N, \varepsilon_{AA}, \varepsilon_{BB}, \varepsilon_{AB}) = \exp\left(\frac{Nzg}{2}\right) Z(\omega, \Delta\tilde{\mu}; N) \tag{10}$$

where $g \equiv -(\varepsilon_{AA} + \varepsilon_{BB})/2kT$ depends trivially on the temperature, and $Z$ is the configurational partition function, whose value does not depend on the absolute values of the pair interactions, $\varepsilon_{AA}$, $\varepsilon_{BB}$ and $\varepsilon_{AB}$, but only on their relative values as measured by the exchange energy $\omega$. Here

$$Z(\omega, \Delta\tilde{\mu}; N) \equiv \sum_{\text{config}} \exp \mathscr{H} \tag{11}$$

where $\mathscr{H}$, the dimensionless Hamiltonian, is given by

$$\mathscr{H} \equiv -N_{AB}\omega + (N_A - N_B)\Delta\tilde{\mu}. \tag{12}$$

Equations (10)–(12) show that the thermodynamic properties of the simple lattice mixture depend on three dimensionless variables: $\omega$, $\Delta\tilde{\mu}$ and $g$. For example, the previous expression for the mole fraction can be rewritten in terms of these groups as

$$(2x_A - 1) = \frac{1}{N}\left(\frac{\partial \ln Z}{\partial \Delta\tilde{\mu}}\right)_{\omega}. \tag{13}$$

Similarly, the energy of mixing, given by

$$\Delta E_{mix} = E - N_A E_A^{\circ} - N_B E_B^{\circ}$$

where $^{\circ}$ denotes a pure component property, can be expressed, using eqs (5)–(7), in terms of $\langle N_{AB}\rangle$, the average number of nearest-neighbor $AB$ pairs or bonds. $\langle N_{AB}\rangle$, in turn, is obtained by differentiating the partition function

$$\langle N_{AB}\rangle = \left(\frac{\partial \ln Z}{\partial \omega}\right)_{\Delta\tilde{\mu}}. \tag{14}$$

It is easily shown that, in the Ising model at finite temperature, a zero value for the exchange ernergy ($\omega = 0$) results in an ideal solution. On the other hand, $\omega > 0$ produces positive deviations from ideality, so that the mixture becomes unstable at sufficiently low temperatures and exhibits a miscibility gap. Most of the binary mixtures that interest chemical engineers show positive deviations from ideality, and it has been estimated that some 50% show partial immiscibility under typical process conditions (Walas, 1985). Thus, the simple Ising model is an appropriate place to start in an investigation of the potential of RG methods in solution thermodynamics.

RG theory is needed because consolute points in nonideal liquid mixtures are actually mixture critical points, and the thermodynamics of critical points presents unique problems. This fact has emerged from the extensive study of critical phenomena that has been carried out in recent years which demonstrated that the difficulties associated with critical points demand special techniques (Widom, 1965; Stanley, 1971; Domb and Green, 1972–1986; Levelt Sengers and Sengers, 1975, 1981; Moldover and Gallagher, 1978; Fox, 1983; Kumar *et al.*, 1983). Normally, chemical engineers have only passing interest in critical points, but it is being increasingly realized that critical phenomena in liquid mixtures constitute a special case. In fact, the interesting part of the phase diagram in partially miscible mixtures generally includes the critical, or consolute, point. Furthermore, the consolute point influences much of the phase diagram: experiment shows that anomalous critical effects appear in liquid mixtures over a temperature range of $\pm$ 10% of the critical temperature (Kumar *et al.*, 1983); this is equivalent to $\pm 30^{\circ}$C if the consolute point occurs at room temperature. [In contrast, vapor liquid equilibrium calculations are normally carried out at conditions far removed from the critical point so that nonclassical effects can be ignored. Even for processes, such as supercritical extraction, that are based on critical phenomena, classical equations of state can often be used to describe the phase equilibria of simple systems to within engineering accuracy (Paulaitis *et al.*, 1983; Penninger *et al.*, 1985; McHugh and Krukonis, 1986; Squires and Paulaitis, 1987). However, even here when the phase diagram is complicated—by the presence, for example, of a region of liquid–liquid equilibrium near the solvent critical point—the modern theory of critical phenomena may be required.] Having introduced the Ising model as a simple model of a nonideal liquid mixture, attention will be now focused on ways of obtaining its properties while taking critical phenomena into account.

## 4. REAL-SPACE RENORMALIZATION GROUP THEORY

Except in the trivial case of an ideal mixture ($\omega = 0$), the partition function, $Z$ [eq. (11)], cannot be computed exactly in closed form. Most of the approximations introduced in the process of estimating $Z$ are of the so-called classical type. The classical analysis of critical behavior assumes that the thermodynamic potential is an analytic function, which can be expanded in a Taylor series about the critical point (Stanley, 1971). Normal thermodynamic stability criteria (Modell and Reid, 1983) eliminate some of the terms in the expansion, and the remaining non-zero terms give the asymptotic critical behavior. This analysis predicts that the behavior of a pure fluid or multicomponent mixture in the vicinity of a vapor–liquid or liquid–liquid critical point can be characterized by *critical exponents*. Experimentally, these are known to be the same in all pure fluids and binary mixtures regardless of the substances involved (Kumar *et al.*, 1983), and in fact the classical asymptotic expansion predicts specific universal values. Most of the statistical mechanical methods, such as quasichemical theory, that are currently used in applied molecular thermodynamics predict the same *classical* values for the critical exponents. Unfortunately, the classical predictions disagree strongly with experimental data (Kumar *et al.*, 1983), which shows that the assumption of analytic behavior is not justified. This failure of the classical methods is now widely appreciated by chemical engineers (Eckert *et al.*, 1980). Work over the last 20 years has shown that the disagreement with experiment is directly attributable to the approximations in the method of obtaining $Z$ (or to the analyticity assumption) rather than to the model itself. Indeed, the Ising model is known from series expansions to have the correct nonanalytic critical behavior (Domb, 1974).

Since classical exponents result from using an analytic method of analysis and not from the model, it is not possible to use effective parameters in the model to compensate for the incorrect asymptotic critical behavior. Until recently the only methods available that yielded the true nonanalytic behavior were graphical series expansion and direct computer simulation. Since modeling the correct critical behavior is vital for accurate predictions of important thermodynamic properties, such as the shape of the miscibility curve, it is unfortunate that neither of these methods is suitable

for engineering calculations. However, a practical nonanalytic approach has been developed in the form of RG theory.

Basically, the RG defines a transformation between the system of interest and another whose partition function can be more easily obtained (Burkhardt and Leeuwen, 1982). The transformation *renormalizes* the interactions (i.e. the parameters in the partition function) without changing the form of the Hamiltonian. Usually, this renders $\mathcal{Z}$ easier to calculate. If $\mathcal{Z}$ remains intractable even after the transformation, then the transformation is applied repeatedly until, eventually, it maps the original system onto a trivial system. In theory, this can be achieved by removing some of the degrees of freedom of the system in each iteration, so that, eventually, the system is small enough to be treated explicitly ($N \approx 1$). In practice, the parameters in the Hamiltonian rapidly take on trivial renormalized values so that even infinite systems can be handled explicitly. Note that if a value for the original partition function is to be obtained, the transformation must not only relate the Hamiltonian parameters, $\Delta\tilde{\mu}$ and $\omega$, to their renormalized values, $\Delta\tilde{\mu}'$ and $\omega'$, but, in addition, it must relate the partition functions, $\mathcal{Z}$ and $\mathcal{Z}'$, of the two systems.

Renormalization theory first appeared 30 years ago in the work of Dyson, Gell-Mann, Low and others on quantum electrodynamics (Amit, 1984). In its applications to critical phenomena, developed over the last decade and a half, RG theory has two main branches: the *momentum-space* renormalization group and the *real-space* renormalization group. Although momentum-space methods have yielded some of the most general and accurate RG results, they will only be briefly discussed here because the real-space methods are of greater practical importance. In the momentum-space method the Fourier transform of the partition function is manipulated (Ma, 1976; Huang, 1987). This approach has proven particularly useful for determining the values of the universal properties, i.e. those properties, such as critical exponents, whose values are common to many different systems. Momentum-space RG theory predicts the values of these exponents to within experimental error, in contrast to the older classical theories, which gave large systematic errors in the exponents. However, momentum-space methods are not normally used to predict nonuniversal properties, such as the global shape of the coexistence curve, because the details of the Hamiltonian which determine such properties are dropped in the calculation. In contrast, real-space RG methods always operate on the complete Hamiltonian [eq. (12)] and thus yield predictions for the entire phase diagram and not just the asymptotic critical region. In the remaining sections only these practical renormalization techniques will be considered. The momentum-space renormalization group method is discussed in detail by Wilson and Kogut (1974), Brezin *et al.* (1976) and Amit (1984).

As the critical point in a pure fluid is approached, density fluctuations grow rapidly. This gives rise to a strong scattering of light—the phenomenon known as critical opalescence. An analogous situation occurs in a liquid mixture at the critical solution point; the composition correlation length diverges to infinity (Fisher, 1964; Münster, 1966; Stanley, 1971). Consequently, large-scale composition fluctuations dominate the behavior of the mixture. This means that, in order to obtain a good approximation to the partition function, a large system must be considered. In fact, the breakdown of the classical theories is due entirely to their neglect of these long-range correlations. In contrast, the RG explicitly takes into account all length scales (Kadanoff, 1976a; Wilson, 1979), leading to better predictions for critical and coexistence behavior. The real-space renormalization techniques that have been developed over the last decade include those shown in Table 2. To date these techniques have been developed mainly for lattice models; fortunately, as mentioned earlier, most correlations for the excess properties of liquid mixtures are also based on lattice models. Thus, without changing the basic models used in engineering molecular thermodynamics, it may be possible to use RG techniques to predict the model properties with greater accuracy. Of the specific techniques listed in Table 2, the MK renormalization group is perhaps the most easily implemented and most widely used. It will be considered in detail in the later sections as a specific example of a RG method. However, the *site–cell* RG method will first be used to illustrate the fundamental ideas behind the real-space renormalization group. Readers primarily interested in the details of the MK technique can proceed directly to Section 6.

Table 2 also lists the *phenomenological* renormalization group. Developed by Nightingale (1982), this method yields accurate results that can be systematically improved. It is based on the fact that the correlations between molecules on a two-dimensional lattice of finite width and infinite length can be calculated exactly by standard statistical mechanical techniques (Huang, 1987). By considering the behavior of the correlation functions on a strip of lattice sites as its width varies, a renormalization relation can be

Table 2. Real-space RG techniques

| General technique | Specific method |
|---|---|
| Site–cell renormalization | Simple finite lattice |
| | Cumulant approximation |
| | Cluster approximations |
| Bond-moving renormalization | Migdal–Kadanoff |
| Phenomenological renormalization | Semi-infinite lattice |

developed. The method has been applied to two-dimensional models with considerable success, but, although in principle it can be extended to three-dimensional lattices, it has been found impracticable to do so. Consequently, the phenomenological RG is more appropriate for studying two-dimensional adsorbed fluids than three-dimensional liquid mixtures. For this reason, and because the method is closely related to finite-size scaling ideas that are independent of the renormalization group, it will not be considered further.

## 5. SITE CELL RENORMALIZATION

The original motivation for developing the site–cell transformation was given by Kadanoff (1966), who started from the fact that in the vicinity of a critical solution point long-range composition correlations occur. The physics of the critical point are dominated by these long-range effects. This being so, Kadanoff argued that a local change in details would not affect the critical behavior. He suggested that the three-dimensional lattice be divided into *cells* of $2^3$ sites, and he argued that near the consolute point it is reasonable to average over all configurations in the cell because the correlation length is much larger than the cell dimensions. Each cell is replaced by a single site, which will be occupied by a molecule of type $A$ or $B$, depending on whether the sites in the cell were originally predominantly occupied by $A$ or $B$. The array of cells then becomes an array of sites that is structurally equivalent to the original lattice, but with an increased lattice spacing. Molecules on these sites interact via new, *rescaled*, or *renormalized* energies. Kadanoff used this rescaling idea to derive the scaling laws of critical behavior that Widom (1965) had previously proposed on an empirical basis. Neimeijer and Leeuwen subsequently developed Kadanoff's idea into a practical renormalization method (1973, 1974, 1976). The particular site–cell renormalization technique known as the *majority rule* is shown schematically in Fig. 1 for a two-dimensional lattice.

Suppose that $\underline{x}$ denotes the configuration of the original lattice, i.e. the species assignment of every site, and that $\underline{x}'$ denotes the configuration of the renormalized lattice. Then, if the partition function was initially expressed as a sum over all possible $\underline{x}$, after the

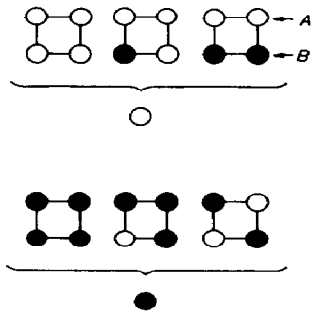


Fig. 1. Possible site-cell renormalization rule. A *majority rule* determines whether a cell of four molecules in a planar square lattice will be replaced by a single $A$ or $B$ molecule.

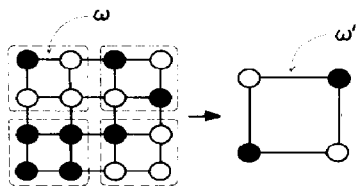


Fig. 2. Renormalization of a planar lattice. The configuration of the original lattice is denoted by $\underline{x}$ and that of the renormalized lattice by $\underline{x}'$; many different $\underline{x}$ will yield the same $\underline{x}'$. If the partition function is to be preserved in the transformation the exchange energy $\omega$ must change, i.e. it must be renormalized.

renormalization transformation it is given by a sum over all possible $\underline{x}'$. Notice, that many different $\underline{x}$ will reduce to the same $\underline{x}'$; this should be clear from Figs 1 and 2. At this point, Kadanoff's argument is used to relate the old and new systems; that is, it is required that the partition function be preserved in the transformation, at least up to a trivial constant. For this to hold in general, the parameters of the Hamiltonian must be allowed to change. In the case of the Ising example, the requirement of preserving the partition function leads to the renormalization of $\omega$ and $\Delta\tilde{\mu}$. The new Hamiltonian, $\mathscr{H}'$, is defined by demanding that it satisfy the *renormalization rule*

$$K' \exp[-\mathscr{H}'(\underline{x}')] = \Sigma \exp[-\mathscr{H}(\underline{x})] \qquad (15)$$

where the summation is only over those $\underline{x}$ that contribute to the given $\underline{x}'$. In eq. (15) the left-hand side is clearly the contribution to the partition function of the renormalized sites—after the transformation. Likewise, the right-hand side is the contribution of the original cells—before the transformation. The term $K'$ is introduced to permit a convenient normalization of the new Hamiltonian. Recall that the exchange energy, $\omega$, was defined so that in eq. (12) only the number of unlike interactions, $N_{AB}$, appeared in the Hamiltonian. After renormalizing the lattice all effective interactions ($AA$, $AB$, $BB$) will, in general, have nonzero values. To reexpress $\mathscr{H}'$ in terms of a single effective interaction, as in eq. (12), $\varepsilon_{AA}$ and $\varepsilon_{BB}$ must again be removed from within the summation. This generates the term $K'$ where

$$K' = \exp(N' z g'/2).$$

Equation (15) can be rewritten as a sum over *all* configurations $\underline{x}$ by introducing a weighting—or projection—function, $P(\underline{x}, \underline{x}')$. For example, for the renormalization rule described above (the majority rule of Fig. 1), $P(\underline{x}, \underline{x}')$ is unity if $\underline{x}$ contributes to $\underline{x}'$ and zero otherwise. In this manner, the renormalization rule becomes

$$K' \exp[-\mathscr{H}'(\underline{x}')] = \sum_{\underline{x}} P(\underline{x}, \underline{x}') \exp[-\mathscr{H}(\underline{x})]. \qquad (16)$$

The weight function $P$ is the quantitative expression of the chosen renormalization rule. For example, in some renormalization schemes not all the $\underline{x}$ leading to a given $\underline{x}'$ need contribute with equal weights and this

can be taken into account by a suitable expression for $P$. It is also possible to consider renormalization prescriptions in which a given original configuration $\underline{x}$ contributes in part to a certain $\underline{x}'$ (say $\underline{x}'_1$) and in part to another $\underline{x}'_2$). In fact, the only restriction on $P$ (other than that it be positive) is that the partition function be conserved by the RG step. This is achieved by demanding that

$$\sum_{\underline{x}'} P(\underline{x}, \underline{x}') = 1 \tag{17}$$

for then

$$\begin{aligned} K'Z' &= \sum_{\underline{x}'} K' \exp(\mathscr{H}') \\ &= \sum_{\underline{x}'} \sum_{\underline{x}} P(\underline{x}, \underline{x}') \exp[\mathscr{H}(\underline{x})] \\ &= \sum_{\underline{x}} \left[ \sum_{\underline{x}'} P(\underline{x}, \underline{x}') \right] \exp(\mathscr{H}) \\ &= \sum_{\underline{x}} \exp(\mathscr{H}) \\ &= Z. \end{aligned}$$

Apart from eq. (17) the choice of weight function $P$, i.e. of renormalization rule, is arbitrary, with different choices giving rise to different real-space RG methods. Having defined $P$, eq. (16) must be solved for the renormalized Hamiltonian. Unfortunately, evaluating the right-hand side of this equation is of comparable difficulty to calculating the partition function directly; further simplifications are obviously necessary. Nevertheless, this approach *does* have an important advantage over mean-field theories: the approximations that will be introduced below will not preclude nonanalytic behavior. In fact, the renormalization mechanism itself will generate the desired nonanalytic critical behavior.

Of the various site–cell RG techniques the simplest to define and implement is the *finite-lattice* RG, in which the infinite lattice is approximated by a finite (and small) sublattice in the calculation of the RG transformation (Nauenberg and Nienhuis, 1974a, b; Tjon, 1974; Subbarao, 1975). This approximation is introduced because it is relatively easy to numerically evaluate the summation on the right-hand-side of eq. (16) for a small lattice of, say, eight or even 16 sites. Although the resulting relationship between the original and the renormalized interactions has been derived from a finite lattice, it is assumed to also hold for the renormalization of the infinite lattice. Figure 3 represents schematically a 16-site, two-cell transformation of a simple cubic lattice. In this technique there is a trade-off between the accuracy obtained and the effort required: generally speaking, the larger the number of sites in the finite lattice, the better the results but the more difficult the summation. However, because of the RG structure, even crude approximations will lead to nonanalytic critical behavior. Indeed, the RG structure is needed to obtain any phase

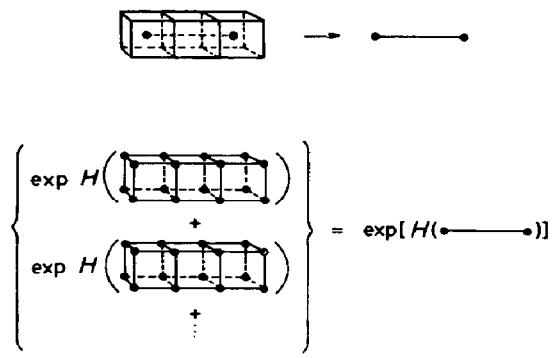


Fig. 3. Simple finite-lattice transformation. There are two cells and each cell contains eight old sites and one new site. The equation shown schematically represents the calculation of the renormalized interaction between two $B$ molecules. Therefore, only those configurations of the original cells that lead to the two $B$ molecules (as specified by a chosen renormalization rule) will contribute terms to the sum, which is easily evaluated on a computer.

separation; a Monte Carlo simulation or direct evaluation of the partition function of a finite lattice of this size would fail to show any critical behavior at all (Binder, 1979, 1983).

Since the renormalized sublattice shown in Fig. 3 consists of only two sites, its Hamiltonian can only contain single-site and nearest-neighbor interactions. Four distinct configurations are possible on the two sites that represent the renormalized lattice and, consequently, eq. (16) actually yields four independent equations. This corresponds to the number of unknown parameters in the renormalized Hamiltonian: three types of pair interaction, and a chemical potential field parameter. Thus $\mathscr{H}'$ is well defined and is of the same type as $\mathscr{H}$. However, if a larger finite lattice is used in the interest of accuracy, together with the same $2 \times 2$ majority spin renormalization rule, then, because of the larger number ($> 4$) of possible configurations on the new sublattice, more equations will be generated than there are parameters in the original Hamiltonian. Physically speaking, this means that, to avoid overdetermination, the renormalized Hamiltonian must have extra types of interaction that are not present in the original Hamiltonian. For example, in the 16-site, four-cell approximation for the two-dimensional Ising model, it is found that next-nearest-neighbor and four-site interactions are generated in addition to the renormalized single-site and nearest-neighbor terms. In fact, although for any simple finite-lattice RG there will be a maximum set of possible interactions, if eq. (16) was solved exactly for the full lattice the number of interactions would increase with each iteration. Thus, the RG transformation usually generates long-range interactions. This is normally handled by truncation whereby terms other than the simplest are ignored (Neimeijer and Leeuwen, 1976). Notwithstanding this truncation, reasonable results are obtained in the simple finite-lattice method, although convergence is slow with increasing numbers of cells.

Table 3. Critical properties of the simple cubic Ising model from exact, mean-field, and real-space RG methods; the dimensionless temperature is defined by $T^* \equiv 2/\omega$

| Method | $T_c^*$ | $\beta$ | $\nu$ |
|---|---|---|---|
| Series (exact) | 4.51 | 0.32 | 0.64 |
| Quasichemical | 4.93 | 0.50 | 0.50 |
| O(1) $2 \times 2 \times 2$ cumulant RG | 3.36 | 0.17 | 0.80 |
| O(2) | 4.05 | 0.40 | 0.81 |
| O(3) | 4.42 | 0.40 | 0.81 |
| Two-cell cluster RG | 3.28 | 0.16 | 0.82 |
| Migdal–Kadanoff RG | 15.27 | 0.47 | 1.06 |
| Kadanoff variational RG | 4.18 | 0.32 | 0.63 |

The *cumulant expansion* (Neimeijer and Leeuwen, 1974; Hsu *et al.*, 1975; Kadanoff and Houghton, 1975) and *cluster approximation* (Neimeijer and Leeuwen, 1973) represent two other classes of widely used real-space RG techniques. In contrast to the finite-lattice RG, which is an unsophisticated low-temperature technique, the cumulant expansion is an accurate high-temperature method and the cluster approximation is applicable at all temperatures. Typical results for the simple Ising model are shown in Table 3. Table 3 shows the critical exponents $\beta$, which determines the curvature of the coexistence curve near the consolute point in a partially miscible binary liquid mixture (Fig. 4), and $\nu$, which determines the rate of divergence of the fluctuation correlation length at the consolute point (Stanley, 1971). Unfortunately, although the cumulant and cluster values represent an improvement over the classical estimates, practical difficulties arise in using these methods. For example, the cumulant expansion seems to be, at best, asymptotically convergent for a given cell size (Hsu *et al.*, 1975), and the convergence of the cluster approximation is found to be so slow that the method is essentially restricted to two-dimensional lattices (Neimeijer and Leeuwen, 1976).

## 6. BOND-MOVING RENORMALIZATION

In this section the MK renormalization group is considered in detail. Like the other transformations listed in Table 2, it is an approximate technique that gives reasonably quantitative results; the MK method, however, is particularly easy to implement. The basic idea was introduced by Migdal (1976), but Kadanoff (1976b) and Maris and Kadanoff (1978) reformulated the theory in a *bond-moving* terminology that simplifies the interpretation of the method.

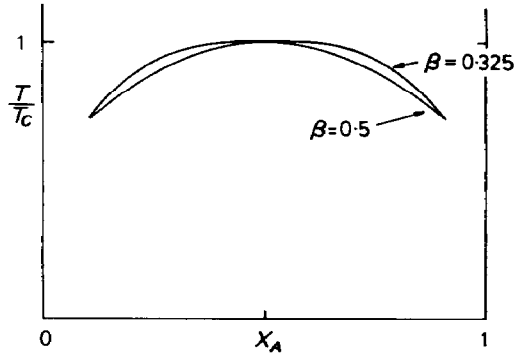


Fig. 4. Liquid–liquid coexistence curve for a simple binary mixture. Shown are the asymptotic shapes of the curves resulting from different values of $\beta$. For the Ising model $\beta$ has an exact value of 0.3125.

Recall that eq. (12) gives the configurational Hamiltonian in terms of a nearest-neighbor pair interaction (arising from each unlike interaction, or $AB$ bond) and a molecular chemical potential term (from each site in the lattice). Jose *et al.* (1977) pointed out that the Hamiltonian can be formally rewritten by distributing each (site) potential term among the incident bonds at the site. That is, the potential term is dropped but the pair interaction strengths are adjusted to compensate. The lattice relationships give

$$(N_A - N_B) = 2(N_{AA} - N_{BB})/z$$

and eq. (12) becomes

$$\mathscr{H} = -N_{AB}\omega + N_{AA}(2\Delta\tilde{\mu}/z) + N_{BB}(-2\Delta\tilde{\mu}/z) \tag{18}$$

$$= \sum_{nn} \mathscr{H}_{nn} \tag{19}$$

where $\mathscr{H}_{nn}$ represents a *nearest-neighbor bond Hamiltonian*, which takes values depending on the pair type, as shown in Table 4. Having expressed the entire Hamiltonian in a bond form, Kadanoff used a bond-moving step to restructure the lattice. This is shown in

Table 4. Nearest-neighbor bond Hamiltonian, $\mathscr{H}_{nn}$, for the binary liquid mixture Ising model

| $i$–$j$ | $\mathscr{H}_{nn}$ |
|---|---|
| $A$–$A$ | $2\Delta\tilde{\mu}/z$ |
| $A$–$B$ | $-\omega$ |
| $B$–$B$ | $-2\Delta\tilde{\mu}/z$ |

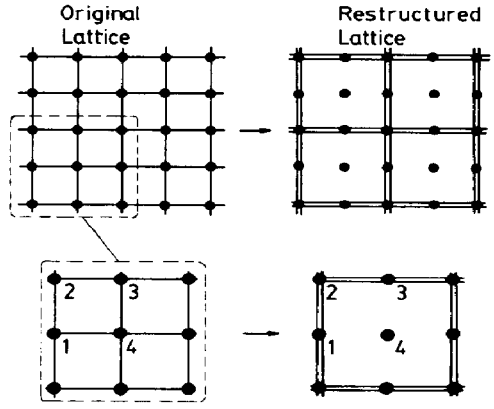


Fig. 5. Bond-moving step in the MK renormalization group for a two-dimensional square lattice. Note that each cell on the restructured lattice has one totally coupled site, two ($d = 2$) partially coupled sites, and one ($= 2d - 1 - d$) totally decoupled site. After bond-moving the effect on the partition function of the interactions between molecules on sites 1 and 4 is approximated by strengthening (doubling) the interactions between molecules on sites 2 and 3, and so on.

Fig. 5, where, for clarity, it is illustrated for a square lattice; the extension to a three-dimensional simple cubic lattice is obvious. Notice that every other line of bonds (i.e. pairwise interactions) is displaced by one lattice spacing. Moving the 1–4 bond in Fig. 5 to coincide with the 2–3 bond simply means that the contribution of the former will be added to that of the latter, which is now effectively doubled, for each configuration of the lattice. Thus, the total number of bonds is conserved. This bond-moving is obviously an approximation because the species that occupy sites 2 and 3 need not always be identical to those occupying 1 and 4. Kadanoff assumed, however, that the partition functions, $Z$, for the original lattice, and $Z_{rst}$, for the *restructured lattice*, are essentially equal. This approximation is responsible for all the error in the method, but it is not completely arbitrary, as will be shown later. Kadanoff was motivated to make this approximation because now the right-hand-side of eq. (16) is easily evaluated, as will be seen below.

The restructured lattice of Fig. 5 appears more complex that the original. However, because it is less connected it can be easily simplified in an exact manner. Notice that the sites of the restructured lattice can be divided into three classes: sites that are decoupled from their nearest neighbors and from the chemical potential field; sites that are partially coupled in a linear arrangement of bonds; and totally coupled sites. This distinction can also be made for the 3-$d$ restructured lattice, and the discussion that follows concentrates on the three-dimensional case. The bond-moving step for a simple cubic lattice is shown in Fig. 6. The relative ratio of decoupled, partially coupled, and totally-coupled sites is just 4:3:1, for a total of eight sites in a $2^3$ cell. Consider the partition function of the restructured lattice. The sites that are totally decoupled from their nearest neighbors simply contribute a factor of $2^{N/2}$ to the partition function, because there are $N/2$ such sites (four out of each cell of eight sites), and each can be occupied in two ways. Since the occupying molecule "sees" no nearest neighbors, there are no energies to consider. Thus, their contribution of $2^{N/2}$ can be explicitly included, and this fraction of the original sites can be ignored from now on. A comparison of Fig. 6(b) and 7(a) shows the effects of this *decimation*.

A further simplification is now possible. The edges

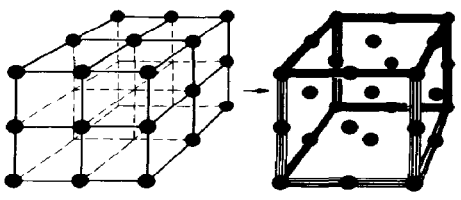

Fig. 6. Restructuring step ($b = 2$) for a cubic lattice. Note that there are now four bonds between each primary and secondary site to compensate for those removed elsewhere. In each cell there are four totally decoupled sites, three partially coupled secondary sites, and one totally coupled primary site.

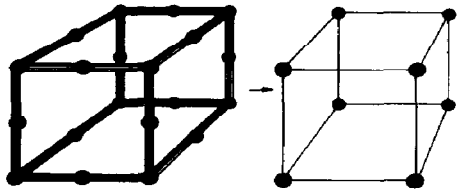

Fig. 7. Renormalized cubic lattice. The eight bonds in the edge of an old, *restructured* cell are replaced by an effective or *renormalized* bond in the new lattice.

of each $2 \times 2 \times 2$ cell on the restructured lattice consist of two *primary* sites separated by a *secondary* site which is connected to each primary site by four bonds. The key point in the MK renormalization group is that the multiple bonds and secondary site can be replaced, without error, by a single effective bond between the primary sites. The resulting *renormalized lattice* is shown in Fig. 7(b). Note that it has exactly the same connectivity as the original lattice [Fig. 6(a)] but the lattice spacing has been increased by a factor of two. In the notation of Section 5, $\underline{x}$ corresponds to a configuration on the original lattice (or more precisely, on the restructured lattice), $\underline{x}'$ corresponds to a configuration on the primary sites, and the renormalization rule is that $P(\underline{x}, \underline{x}') = 1$ if the configuration of primary sites in $\underline{x}$ is given by $\underline{x}'$, and $P = 0$ otherwise, so that the summation is effectively over all non-primary sites.

The strength of the effective bond that replaces both the partially coupled site and the multiple bonds is determined as follows. Consider one edge of the cell in Fig. 7(a), and its contribution to the partition function. Suppose that the primary sites are both occupied by $A$ molecules. Then, before renormalization the multiple bonds of the edge make a different contribution for each occupation of the secondary site

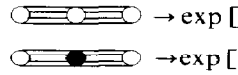

$$\rightarrow \exp[8(2\Delta\tilde{\mu}/z)]$$

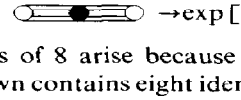

$$\rightarrow \exp[8(-\omega)].$$

The factors of 8 arise because each of the configurations shown contains eight identical bonds. As shown in Table 4, the bond Hamiltonian for each $AA$ pair is $2\Delta\tilde{\mu}/z$ and $-\omega$ for each $AB$ pair.

After renormalization, this same cell edge makes a single contribution to the partition function of

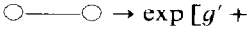

$$\rightarrow \exp[g' + (2\Delta\tilde{\mu}'/z)].$$

The new, effective, or renormalized, parameters have been designated by primed quantities. Note that $g'$ is the normalization factor per bond.

In order that the partition function be conserved, the sum of the two terms from the old configurations must equal that of the renormalized bond, giving

$$\exp(g' + 2\Delta\tilde{\mu}'/z) = \exp(16\Delta\tilde{\mu}/z) + \exp(-8\omega).$$

Similarly, when the two primary sites are occupied by $B$ molecules, preservation of the partition function yields

$$\exp(g' - 2\Delta\tilde{\mu}'/z) = \exp(-16\Delta\tilde{\mu}/z) + \exp(-8\omega)$$

while for an $AB$ pair it gives

$$\exp(g' - \omega') = \exp(8\Delta\tilde{\mu}/z - 4\omega) + \exp(-8\Delta\tilde{\mu}/z - 4\omega).$$

These equations can be rearranged to give explicit expressions for the renormalized parameters

$$\omega' = \ln\left[\frac{\cosh^{1/2}(4\omega + 8\Delta\tilde{\mu}/z)\cosh^{1/2}(4\omega - 8\Delta\tilde{\mu}/z)}{\cosh(8\Delta\tilde{\mu}/z)}\right] \tag{20}$$

$$\Delta\tilde{\mu}' = 4\Delta\tilde{\mu} + \frac{z}{2}\ln\left[\frac{\cosh(4\omega + 8\Delta\tilde{\mu}/z)}{\cosh(4\omega - 8\Delta\tilde{\mu}/z)}\right] \tag{21}$$

$$g' = -4\omega + \frac{1}{2}\ln[4\cosh(4\omega + 8\Delta\tilde{\mu}/z)\cosh(4\omega - 8\Delta\tilde{\mu}/z)]. \tag{22}$$

Equations (20)–(22) are of central importance in the MK method as applied to the simple binary model and are known as the *recursion relations*. Note that the parameters always appear in dimensionless form.

## 7. RENORMALIZATION OF THE PARTITION FUNCTION

The transformation discussed in the previous section had the net effect of relating the original lattice [Fig. 6(a)], to the final lattice [Fig. 7(b)]. Both have the same connectivity, but the new lattice has twice the spacing and fewer numbers of sites and bonds—the desired simplification. Their respective parameters are $(\omega, \Delta\tilde{\mu})$ and $(\omega', \Delta\tilde{\mu}')$, related by eqs (20)–(22). It is a normal feature of the MK renormalization group that the analysis leading to the recursion relations is quite straightforward. For this reason the method has been extensively used to study the critical properties of a wide range of models (Burkhardt and Leeuwen, 1982).

Equations (11) and (12) define the configurational partition function of the original lattice in terms of $\omega$ and $\Delta\tilde{\mu}$. The partition function of the renormalized lattice is given by an analogous expression with "primed" quantities

$$Z' = \sum_{\text{config}} \exp[-N'_{AB}\omega' + (N'_A - N'_B)\Delta\tilde{\mu}'].$$

The summation is taken over all configurations on the primary sites of Fig. 7(b). Taking into account how the transformation was constructed, $Z$ can be related to $Z'$ as follows. The transformation from Fig. 6(a) to Fig. 6(b) conserves the partition function (albeit only approximately)

$$Z_{\text{rst}} \approx Z. \tag{23}$$

Furthermore, the transformation from Fig. 7(a) to Fig. 7(b) relates the restructured and renormalized partition functions, $Z_{\text{rst}}$ and $Z'$, by

$$Z_{\text{rst}} = K'Z' \tag{24}$$

where $K'$, defined as follows:

$$K' = 2^{N/2}\exp\left(\frac{N'zg'}{2}\right)$$

accounts for the decoupled sites—each generating a factor of $2^{N/2}$—and for the normalization constant associated with each new effective bond; since there are $N'z/2$ renormalized bonds and each generates a constant, $g'$, the normalization constant for the entire lattice is $(N'z/2)g'$.

The primary goal is to determine the unknown partition function, $Z$, since from it all other thermodynamic properties can be calculated. From eqs (23) and (24), $Z$ is related to $Z'$ by

$$Z = 2^{N/2}\exp[(N'z/2)g']Z' \tag{25}$$

but, of course, $Z'$ is also unknown. The next section shows how the iterative application of eqs (20)–(22) and (25) effectively leads to the calculation of $Z$.

The two sides of eq. (25) do not correspond to distinct lattices, because $Z'$ simply represents the fraction of the original lattice ($N' = N/8$) left after the partial summation. Accordingly, there should be no discontinuity between the physical behavior of the two systems; their thermodynamic states should be qualitatively similar. Thus, if the original system is in a state of two-phase coexistence or is at its consolute point, then the renormalized system should also show phase-separation or be at its critical point. This is the physical significance of Kadanoff's idea that local changes do not afffect the qualitative thermodynamic properties if the correlation length is large. The behavior of the recursion relations supports this physical intuition, as will be seen in Section 9.

Recall that only the bond-moving step (Figs 5 and 6) involves an approximation. Burkhardt and Leeuwen (1982) have described the qualitative effect of this approximation on the partition function as follows. If every other line of bonds is moved as in Fig. 5, the original Hamiltonian is changed—perturbed—from $\mathscr{H}(\underline{x})$ to $\mathscr{H}(\underline{x}) + \mathscr{V}(\underline{x})$. The restructured lattice partition function is given exactly by

$$Z_{\text{rst}} = \sum_{\underline{x}} \exp[\mathscr{H}(\underline{x}) + \mathscr{V}(\underline{x})]. \tag{26}$$

The explicit form of the perturbation $\mathscr{V}(\underline{x})$ will be discussed below. Notice that eq. (26) can be written as

$$Z_{\text{rst}} = \sum_{\underline{x}} [1 + \mathscr{V}(\underline{x}) + \tfrac{1}{2}\mathscr{V}(\underline{x})^2 + \ldots]\exp[\mathscr{H}(\underline{x})].$$

Since $\exp(a) \geq (1 + a)$, truncation after the linear term yields the inequality

$$Z_{\text{rst}} \geq \sum[1 + \mathscr{V}(\underline{x})]\exp[\mathscr{H}(\underline{x})] = (1 + \langle\mathscr{V}\rangle_{\mathscr{H}})Z \tag{27}$$

where the mean perturbation is given by

$$\langle\mathscr{V}\rangle_{\mathscr{H}} = Z^{-1}\Sigma\mathscr{V}\exp(\mathscr{H}).$$

To see the specific form of the bond-moving perturbation, consider the lattice shown in Fig. 5. For any particular configuration, the perturbation introduced by moving the single bond 1–4 onto bond 2–3 will clearly be given by

$$\mathscr{V} = -\mathscr{H}_{nn}(1,4) + \mathscr{H}_{nn}(2,3)$$

where $\mathscr{H}_{nn}(i,j)$ denotes the dimensionless $i$–$j$ bond Hamiltonian, which depends on the molecular species occupying sites $i$ and $j$ (Table 4). Averaging this perturbation over all configurations gives

$$\begin{aligned}\langle \mathscr{V} \rangle_{\mathscr{H}} &= \langle -\mathscr{H}_{nn}(1,4) + \mathscr{H}_{nn}(2,3) \rangle_{\mathscr{H}} \\ &= -\langle \mathscr{H}_{nn}(1,4) \rangle_{\mathscr{H}} + \langle \mathscr{H}_{nn}(2,3) \rangle_{\mathscr{H}} \\ &= 0 \end{aligned} \tag{28}$$

where the fact that averages on the original lattice are translationally invariant has been used. Thus, to first order, the bond-moving perturbation is zero. Although the second term in the expansion, $\langle \frac{1}{2}\mathscr{V}^2 \rangle$, has not been evaluated, eqs (27) and (28) yield the important result

$$Z_{\text{rst}} \geqslant Z.$$

That is, the restructured partition function obtained by the bond-moving process is an upper bound to the original partition function. Furthermore, to first order they are identical. This represents a quantitative justification for the bond-moving approximation. The upper-bound condition that results from a bond-moving step has been used by Kadanoff in a variational calculation that combines features of the site-cell method with the bond-moving ideas (Kadanoff, 1975; Kadanoff and Houghton, 1975; Kadanoff *et al.*, 1976). As is clear from Table 3, this variational method is very successful for the simple binary model. However, the transformation generates long-range interactions so that the parameter space is quite large, even for the Ising model. For all practical purposes, this limits the method to simple models. It will not be considered further here; see Burkhardt and Leeuwen (1982) for further details.

The effect of the MK bond-moving step can be understood in physical terms for various limiting situations. For $\omega > 0$ the mixture will phase-separate at very low temperatures, and the lattice will be occupied almost exclusively by one species. Since the number of bonds has been preserved, and they are all identical ($AA$ or, in the second ground state, $BB$), the procedure becomes exact. The same is true for very large values of the field parameter, $\Delta\tilde{\mu} \to \pm\infty$, because in such cases the lattice is also filled with only one species ($\Delta\tilde{\mu} \to +\infty$ corresponds to $\mu_A \to \mu_A^0$ and $\mu_B \to -\infty$, that is, to $x_B \to 0$). On the other hand, at very high temperatures and zero field complete mixing occurs. But in this limit the interaction energies are no longer significant; the perturbation term in eq. (26) vanishes, because $\mathscr{V}$ represents a reduced perturbation energy, $V/kT$. As a result, at high temperatures the thermodynamic potential is dominated by entropic contributions, which the MK algorithm determines correctly for the Ising model. The accuracy of the bond-moving approximation at intermediate conditions will be considered in more detail in Section 10.

## 8. ITERATIVE RENORMALIZATION

In the previous section, the relationship between $Z$ and $Z'$, the configurational partition functions for the old and new lattices, was given by eq. (25). Equation (25) implicitly relates the thermodynamic properties of the two systems, that is, it implicitly relates the dependent variables. On the other hand, the independent variables—the interaction energies, temperature, and chemical potentials—are explicitly related through eqs (20)–(22). These four equations are now applied iteratively. Notice that $g$ does not appear anywhere on the right-hand-side of eqs (20)–(22). Thus, $g$ is a dependent variable during the iterative application of these equations and need not be considered with the two independent variables $\omega$ and $\Delta\tilde{\mu}$.

When the recursion relations are applied repeatedly, a sequence of parameters is generated:

$$\omega \to \omega' \to \omega'' \to \ldots$$

$$\Delta\tilde{\mu} \to \Delta\tilde{\mu}' \to \Delta\tilde{\mu}'' \to \ldots$$

Physically, this sequence corresponds to successive decimations of the lattice (Fig. 8). A schematic of the evolution of the parameters is shown in Fig. 9. For example, after two decimations (i.e. two applications of the recursion relations) the mixture corresponding to the point $a_0$ will have been transformed into, or mapped onto, the mixture corresponding to the point $a_2$. Although the recursion relations define a finite

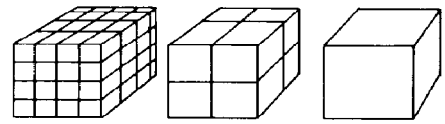

Fig. 8. Effect of successive *decimations* on a simple cubic lattice. The connectivity remains the same (each site is connected by bonds, i.e. interactions, to six nearest neighbors) but the number of sites decreases and the bond strengths are renormalized.

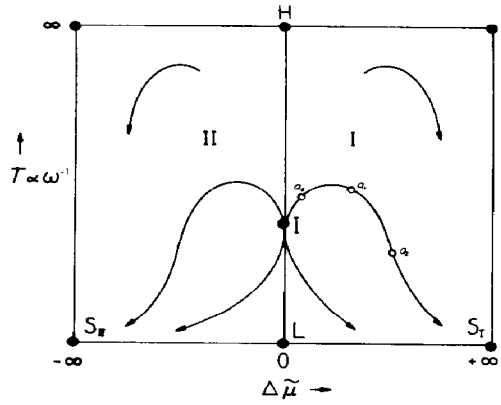


Fig. 9. Evolution of the Hamiltonian parameters $\omega$ and $\Delta\tilde{\mu}$ under the action of the recursion relations. The renormalization transformation defines a discrete mapping but, here, lines have been drawn through the successive points to indicate continuous *flows* in the planar parameter space. Those *fixed* points that do not move under the action of the parameters are indicated by ●. The infinite range of the two parameters has been compressed into the figure by using hyperbolic tangent scales.

rather than differential transformation, a continuous line has been drawn through the successive points to indcate *flows* in the parameter plane. The structure of the flows, i.e. in how a given initial point leads to one or another of the indicated *fixed* points, is of considerable importance (Neimeijer and Leeuwen, 1976; Pfeuty and Toulouse, 1977). This structure is analyzed in the next section; the focus here is on the computation of the partition function and thermodynamic properties.

The repeated application of eq. (25) can be best implemented if it is rewritten as

$$\frac{1}{N}\ln Z = \frac{1}{2}\ln 2 + \frac{z}{2}\frac{g'}{8} + \frac{1}{8}\left(\frac{1}{N}\ln Z\right)'$$

where use has been made of the fact that $N = 8N'$. Thus

$$\begin{aligned}\frac{1}{N}\ln Z &= \frac{1}{2}\ln 2 + \frac{z}{2}\frac{g'}{8} + \frac{1}{8}\left[\frac{1}{2}\ln 2 + \frac{z}{2}\frac{g''}{8}\right. \\ &\quad \left. + \frac{1}{8}\left(\frac{1}{N}\ln Z\right)''\right] \\ &\quad \vdots \\ &= \frac{1}{2}\ln 2 \sum_{n=0}^{\infty}\frac{1}{8^n} + \frac{z}{2}\sum_{n=1}^{\infty}\frac{g^{(n)}}{8^n} \\ &\quad + \lim_{n\to\infty}\frac{1}{8^n}\left(\frac{1}{N}\ln Z\right)^{(n)}.\end{aligned}$$

The last term vanishes as $n \to \infty$, because of the factor of $8^{-n}$ and because $Z^{(n)}$ is analytic everywhere except at the critical point. Notice also that the first term is the sum of a geometric series. Thus

$$\frac{1}{N}\ln Z = \frac{4}{7}\ln 2 + \frac{z}{2}\sum_{n=1}^{\infty}\frac{g^{(n)}}{8^n}$$

where the successive $g^{(n)}$ are readily obtained from eqs (20)–(22). The thermodynamic potential, given by eqs (3) and (10), becomes

$$\begin{aligned}\frac{Y}{Nk} &= \frac{z}{2^g} + \frac{1}{N}\ln Z \\ &= \frac{4}{7}\ln 2 + \frac{z}{2}\sum_{n=0}^{\infty}\frac{g^{(n)}}{8^n}. \qquad (29)\end{aligned}$$

This expression is the major result of the MK method for the cubic lattice. In practice, it is found that the sum on the right-hand side converges very rapidly, so that no more than a few iterations are required to determine $Y$. All the other thermodynamic properties can then be obtained from $Y$ by using the thermodynamic eqs (1) and (2). For example, the thermodynamic properties $x_A$ and $\Delta E_{\text{mix}}$ can be obtained by numerical differentiation of eq. (29). Alternatively, eqs (13) and (14) can be used, and the recursion relation for $Z$ can be analytically differentiated to obtain recursion formulas for $x_A$ and $\Delta E_{\text{mix}}$ (or, equivalently, for $x_A$ and for $\langle N_{AB}\rangle$). These formulas are presented in Appendix A.

## 9. FIXED POINTS OF THE RENORMALIZATION TRANSFORMATION

The recursion relations define a nonlinear transformation in the *parameter space*. Mathematically these equations define a point mapping that is analogous to a discrete dynamical system, with "time" being related to the number of iterations performed. Flows, or trajectories, are generated under successive mappings, as shown in Fig. 9. The structure of the flows in parameter space is determined by the physics of the model. It is found, for example, that the flows possess *fixed points*. These are points $(\omega^*, \Delta\tilde{\mu}^*)$ that are mapped onto themselves under the renormalization transformation. The occurrence of thermodynamic critical points is related to the existence of fixed points of the RG transformation (Kadanoff, 1976; Neimeijer and Leeuwen, 1976). Under the action of the transformation the correlation length $\xi$ is rescaled by a factor $b$, corresponding to the rescaling of the lattice. In the present example $b = 2$ and thus $\xi' = \xi/2$. However, at a critical point $\xi \to \infty$, so even after an RG transformation $\xi' \to \infty$. Thus, the transformation does not affect the critical correlation length. This suggests that critical points should be associated with fixed points as these are the only points in the parameter space unaffected by the transformation.

The recursion formulas are highly nonlinear and may have many fixed points, most of which will be physically uninteresting or trivial, i.e. points at which the values of the parameters are 0 or $\infty$. There is no *a priori* way of knowing whether a particular transformation, such as that given by eqs (20)–(22), will have nontrivial fixed points. However, most renormalization schemes constructed to date have been found to possess interesting fixed points that correspond to the expected physical behavior of the model. In the case of the Ising model, it is known—from mean-field studies, series expansions, and the arguments of Peierls (Huang, 1987)—that the model should possess a critical point for $\omega > 0$. Indeed, a single nontrivial fixed point is found: the point marked **I** in Fig. 9. The flows also possess several other fixed points, or *sinks*, **S**, as shown. There are called sinks because a large fraction of the parameter space is eventually mapped into them. A sink controls the thermodynamic behavior of the region attracted to it because the analytic nature of the RG transformation ensures that the partition function is also analytic in the same region (see Appendix A). Singularities corresponding to phase transitions can only occur at the borders between regions. This means that the parameter space can be divided into regions according to their sinks, and that all systems whose initial point is in a certain region will be in the same qualitative macroscopic state. The point **I** is a separatrix between two regions (along the line **LIH**): if the model is in a state such that its initial point $(\omega, \Delta\tilde{\mu})$ lies along **IH** then it flows to **H** under repeated transformations, while if it lies on **LI** it flows to **L**. Clearly, **H** is a *high-temperature* state as $\omega_{\mathbf{H}} = 0$, while **L** must be a *low-temperature* state since $\omega_{\mathbf{L}}$

$= \infty$. States lying along **LIH** are of special interest because then $\Delta\tilde{\mu} = 0$, which implies that $\mu_A = \mu_B$. On calculating their thermodynamic properties, it is found that between **I** and **H** the mixture has equimolar composition, $x_A = 0.5$, while from **I** to **L** the composition either rises from 0.5 to 1.0 or falls from 0.5 to 0.0—which occurs depends on whether **LI** is approached from region I or region II. Since the $T$–$x_A$ coexistence curve collapses onto a single line in $T$–$\mu_A$ space, it is clear that **LI** is in fact the coexistence line and that **I** is the Ising model consolute point. Points that are initially in region I eventually flow to a low-temperature, high-field sink, $S_I$, as $\Delta\tilde{\mu} \to \infty$, which corresponds to pure $A$ (since $\Delta\tilde{\mu} \propto \mu_A - \mu_B$), while points in region II flow to a low-temperature, pure $B$ state, $S_{II}$. Thus, points in region I represent a single $A$-rich phase, and those in region II represent a $B$-rich phase.

Finally, it can be shown that the asymptotic structure of the flows in the vicinity of the critical fixed point, **I**, is related to the nonanalytic behavior of the thermodynamic properties at the critical solution point. In fact, from a stability analysis of the linearized recursion relations at **I** the critical exponents can be found (see Appendix B). These, together with the value of the critical temperature are shown in Table 3.

## 10. MODIFICATIONS TO THE MIGDAL–KADANOFF APPROXIMATION

As pointed out above, the MK approximation is the simplest RG method to implement. Though it advances beyond the results of classical, mean-field theories, its simplicity comes at the price of quantitative accuracy, at least as compared to more elaborate, computationally demanding RG techniques. However, the MK method can be modified to greatly improve the quantitative results while at the same time retaining the underlying simplicity (Walker and Vause, 1980, 1983; Walker, 1982; Andelman and Walker, 1983; Goldstein and Walker, 1985). Such modifications are essential for the practical application of the MK method and are described in this section. Other attempts to improve the standard MK RG have involved altering the bond-moving pattern (Swendsen and Zia, 1979) and introducing variational parameters into the transformation (Caracciolo, 1981). Since these methods are of rather limited generality they will not be discussed in detail here.

The basic idea considered in this section is to generalize the way in which bonds are strengthened. Instead of increasing their strength as in simple bond-moving, they will be strengthened by a generalized factor $\lambda$, which will be determined by an appropriate criterion. Thus, on the restructured lattice, $\omega$ will be replaced by $\lambda\omega$ wherever it appears. In the examples presented thus far, $\lambda$ has always been assigned the value $2^{d-1}$ (i.e. $\lambda = 2$ for $d = 2$ and $\lambda = 4$ for $d = 3$); this choice guarantees that the total number of bonds in the original and restructured lattices is the same. Choosing $\lambda$ in this way is quite reasonable, and has the further justification of producing a bound on the exact partition function of the system, as shown in Section 7. It must be remembered, however, that this prescription is still only an approximation, and as such is subject to improvement. In fact, since replacing the restructural lattice with a new lattice and renormalized couplings is an exact procedure, it follows that the only flexibility in the MK method is in the bond-moving step, and hence in $\lambda$.

The simplest possible modification is to set $\lambda = \text{constant} \neq 2^{d-1}$ (Walker and Vause, 1980, 1983). The renormalization transformation remains just as before, except that now the quantities, $\omega'$, $\Delta\tilde{\mu}'$ and $g'$ are written as

$$\omega' = \left[\frac{\cosh^{1/2}(\lambda\omega + 8\Delta\tilde{\mu}/z)\cosh^{1/2}(\lambda\omega - 8\Delta\tilde{\mu}/z)}{\cosh(8\Delta\tilde{\mu}/z)}\right] \tag{30}$$

$$\Delta\tilde{\mu}' = 4\Delta\tilde{\mu} + \frac{z}{2}\ln\left[\frac{\cosh(\lambda\omega + 8\Delta\tilde{\mu}/z)}{\cosh(\lambda\omega - 8\Delta\tilde{\mu}/z)}\right] \tag{31}$$

$$g' = -\lambda\omega + \frac{1}{2}\ln\left[\lambda\cosh(\lambda\omega + 8\Delta\tilde{\mu}/z)\cosh(\lambda\omega - 8\Delta\tilde{\mu}/z)\right] \tag{32}$$

explicitly displaying the $\lambda$ dependence. Note that the original relations for three dimensions, eqs (20)–(22), are recovered when $\lambda = 4$. All the calculations presented in the previous sections can be repeated; clearly the results for transition temperatures, critical exponents and thermodynamic functions, such as the composition $x_A$, will vary continuously with $\lambda$. Note, in comparing eqs (30)–(32) with eqs (20)–(22) that the variable-strengthening parameter $\lambda$ has only been introduced for $\omega$, and not for $\Delta\tilde{\mu}$. In fact, it can be shown that $\Delta\tilde{\mu}$ must be strengthened by a factor of $2^{d-1}$ in order for $x_A$ to assume nontrivial, finite values; thus the only freedom available is in how $\omega$ is strengthened. With just this single parameter available it is not possible to correct all aspects of a given calculation simultaneously; still, definite improvements can be made. For example, it may be of interest, in certain problems, to have accurate values for transition temperatures, or critical exponents. The results for $\omega^*$, the transition temperature, and $\beta$, the coexistence-curve exponent, as functions of $\lambda$ are shown in Fig. 10. In each case the dashed lines indicates the exact value for the three-dimensional Ising model, as well as the result for the unmodified MK calculations. Notice that $\lambda$ must be less than the MK prescrition, $\lambda = 4$, in order to obtain the exact results, indicating that the MK method overstrengthens the bonds. It is clear, then, that a suitable choice for $\lambda$ can increase the quantitative accuracy of the calculation.

The utility of the bond-strengthening parameter is further illustrated in Fig. 11, where the liquid–liquid miscibility curve, for various values of $\lambda$, is compared with exact results for the Ising model. The standard MK calculation is rather poor, but again it can be seen that decreasing $\lambda$ leads to significant improvement. In fact, when $\lambda$ is set to the value 2.3 the exact and

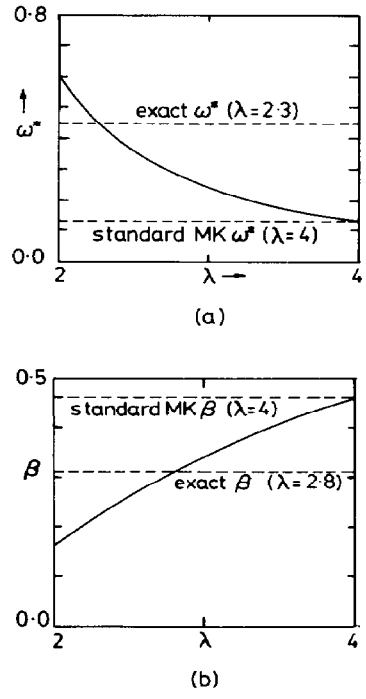


Fig. 10. Critical coupling constant $\omega^*$(a) and $\beta$(b) as functions of the bond-strengthening parameter $\lambda$. Notice that in each case the exact value is obtained by using a smaller value of $\lambda$ than in an unmodified MK calculation.

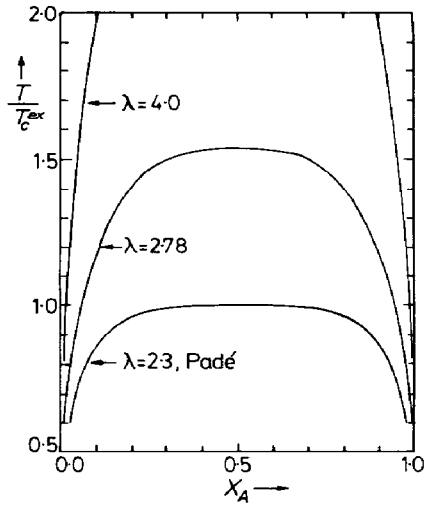


Fig. 11. Composition vs temperature for various values of the bond strengthening parameter $\lambda$, as compared with the exact results. For $\lambda = 2.3$ the exact and approximate curve are essentially identical on this scale. With $\lambda = 2.78$ the exponent $\beta$ takes on its correct value, but the overall composition results are in poor agreement with the exact curve.

approximate curves are virtually indistinguishable on this scale. It should be noted, however, that the exponent $\beta$ is 0.225 in that case; therefore, on an enlarged scale, deviations from the exact results will be visible near the critical point. The accepted value for $\beta$, i.e. 0.3125, can be obtained by choosing the bond-strengthening parameter to be 2.78. The corresponding results, also shown in Fig. 11, give a less satisfactory fit to the full phase diagram. Thus, the appropriate choice for $\lambda$ depends on the particular problem at hand. Different values of $\lambda$, for example, must be used when either the asymptotically critical region or the overall phase diagram is of most interest; for typical applications in solution thermodynamics $\lambda$ would be set to 2.3, the value that best reproduces the overall phase diagram.

With these examples it has been shown that adjusting the bond-strengthening factor can lead to an accurate calculation, though up to this point the focus has been on the Ising model, for which exact results are already known. When faced with a model system which is more complex, it is still possible that exact results will be known for certain special limiting cases. If any exact results are available, $\lambda$ can be calibrated as shown for the Ising model (Walker and Vause, 1983). A specific application of this procedure is discussed in the next section.

Walker and co-workers (Walker, 1982; Andelman and Walker, 1983; Goldstein and Walker, 1985) have presented a more general and powerful approach to improving the MK approximation, an approach based on the notion of preserving the partition function, rather than simply producing a bound to it. As before, the flexibility provided by the bond-strengthening factor is exploited, but now, rather than simply choosing $\lambda$ as a free parameter, it is determined in a systematic way by comparing the partition functions of the original and restructured lattices.

To see how this idea can be put into practice, consider the Ising model with $\Delta\tilde{\mu} = 0$. The first step is to expand the partition function, to lowest nontrivial order, for high and low temperatures, on both the original and restructured lattices. In order to facilitate this expansion, it is useful to redefine the zero of energy, which, of course, has no effect on the statistical mechanics of the system. At present $AA$ and $BB$ bonds correspond to zero energy, $AB$ bonds contribute $-\omega$ (see Table 4); now adding $\omega/2$ to all bonds results in the new bond Hamiltonian

$$\mathscr{H}_{nn} = \begin{cases} \omega/2 & AA \\ \omega/2 & BB \\ -\omega/2 & AB \end{cases}$$

The same Hamiltonian applies for the restructured lattice, except that $\omega$ is replaced with $\lambda\omega$.

First, consider the low-temperature case, $\omega \to \infty$, which is particularly simple since then only two configurations survive: those in which the entire lattice is occupied by one or the other type of molecule. Thus, for the original lattice

$$Z \to 2\exp[3N(\omega/2)].$$

Note that $3N$ is the number of bonds on a cubic lattice

with $N$ sites. For the restructured lattice

$$Z_{rst} \rightarrow 2(2^{N/2}) \exp[(3N/4)(\lambda\omega/2)]$$

where the $2^{N/2}$ contribution from the decoupled sites has been explicitly included. In addition, the restructured lattice has only 1/4 as many bonds as the original; hence the factor of $\frac{1}{4}$. Equating these two limiting expressions yields $\lambda = 4$, in agreement with the MK procedure. Thus the MK approximation is exact at low temperatures.

Next consider the high-temperature limit, where, as will be seen, the MK value for $\lambda$ is no longer exact. At high temperature, $\omega = 0$, all configurations are equally likely. Therefore, both $Z$ and $Z_{rst}$ are simply $2^N$, to lowest order, independent of $\lambda$. Proceeding to higher order in $\omega$ and using standard series expansion methods (Stanley, 1971) it can be shown that

$$Z \rightarrow 2^N[1 + 3N(\omega^2/8)]$$

and

$$Z_{rst} \rightarrow 2^N[1 + (3N/4)(\lambda^2\omega^2/8)]$$

to order $\omega^2$. Equating the thermodynamic potential per site, $Y/N$ and $Y_{rst}/N$, in the limit as $N \rightarrow \infty$ in this case leads to $\lambda = 2$. Thus, in order to preserve the partition function at high temperature the bonds must be strengthened by the square root of the MK value. This conclusion is valid in all dimensions.

It is clear that this procedure can be carried out to higher order, resulting in an increasingly accurate determination of $\lambda$ as a function of temperature. An example is provided by the two-dimensional Ising model, for which the exact partition function can be obtained for both the original and restructured lattices. Equating these partition functions results in the temperature-dependent $\lambda$ shown in Fig. 12 (Walker, 1982); the two dashed lines show the asymptotic high- and low-temperature limits of $\sqrt{2}$ and 2, respectively. The meaning of this result is that if the $\lambda$ given by the solid curve is used, the partition function calculated using eq. (29) agrees with Onsager's exact solution of this problem (Onsager, 1944). Similar results can be obtained in three dimensions, as will be seen below.

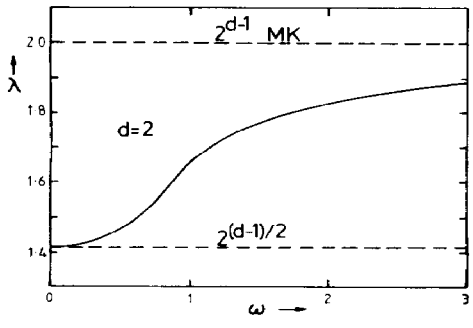


Fig. 12. Bond-strengthening parameter $\lambda$ as a function of the coupling constant $\omega$. Dashed lines represent the asymptotic limits for the high and low temperatures (i.e. small and large coupling, respectively). Note that the MK prescription always overstrengthens the bonds.

Since the determination of a series expansion becomes more difficult at higher orders, this method will be practical only if the low-order results lead to an improvement over MK. This is indeed the case, as can be seen using the following expansions for the three-dimensional Ising model (Andelman and Walker, 1983). For high temperatures

$$Y/Nk = \ln 2 + 3\ln[\cosh(\omega/2)] + 3v^4 + 22v^6$$

where $v = \tanh(\omega/2)$, while on the restructured lattice the corresponding result is

$$Y_{rst}/Nk = \ln 2 + (3/4)\ln[\cosh(\lambda\omega/2)].$$

Both results are correct up to sixth order. The procedure is now as outlined above, where a value for $\omega$ is initially chosen and then $Y_{rst}$ is equated to $Y$, to obtain the corresponding value for $\lambda$. This optimal value of $\lambda$ is used in the recursion relation [eq. (30)] to obtain $\omega'$ for the renormalized lattice. A search is then carried out for a fixed point, and exponents are calculated in the usual way. The results obtained are $\omega^* = 0.474$ and $\nu = 0.637$, as compared to the exact values of 0.443 and 0.638, leading to errors of 7 and 1%, respectively. Similar results are obtained from low-temperature expansions. Recall from Table 3 that the simple MK transformation gave $\omega^* = 0.131$ and $\nu = 1.065$. That is, the critical temperature was in error by more than a factor of three, while the critical exponent was in error by more than 50%. Clearly, low-order expansions of the partition function yield significant improvements. It has been found, however, that further improvement in these results from higher-order terms is very slow, so that the effort involved in calculating longer series is generally not justified.

Another particularly difficult problem associated with the series expansion method is the combining of results obtained from high- and low-temperature expansions. A possible way around this difficulty is to approximate the partition function by calculating it *exactly* on a *finite* lattice. Such a calculation yields a partition function in agreement with exact results up to a certain order, corresponding to the size of the finite lattice, and interpolates with a single functional form between the high- and low-temperature regimes. This modification is based on the same ideas as the series method described above, and gives comparable results, but is simpler and more satisfying to implement. Since this calculation starts on a finite lattice (cluster), and then proceeds with a decimation, it is termed a cluster-decimation approximation (CDA) (Goldstein and Walker, 1985). A simple example for two dimensions is shown in Fig. 13; this will be referred to as a 2 × 2 cluster. A technical point of some importance is that periodic boundary conditions are used on the cluster, as shown in Fig. 13, ensuring that the approximate partition function has the correct low-temperature limit. Part (a) of Fig. 13 shows the 2 × 2 cluster on the original lattice, while in part (b) the

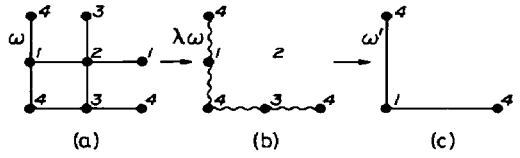


Fig. 13. CDA illustrated for the 2 × 2 cluster. The site numbering indicates the periodic boundary conditions.

corresponding cluster on the restructured lattice is shown.

The first step in the calculation is to determine the partition functions for these clusters. For the original lattice

$$Z = 2\exp(4\omega) + 12 + 2\exp(-4\omega)$$

while on the restructured lattice

$$Z_{\text{rst}} = 4\exp(2\lambda\omega) + 8 + 4\exp(-2\lambda\omega).$$

Setting these expressions equal to one another yields $\lambda$ as a function of $\omega$. In this case $Z$ and $Z_{\text{rst}}$ are simple enough that the result can be expressed analytically, namely

$$\lambda = \frac{1}{2\omega}\ln\left(y + \sqrt{y^2 - 1}\right)$$

where

$$y = [1 + \cosh(4\omega)]/2.$$

Figure 14 shows $\lambda$, using the above result. Note that the correct limits are obtained at both high and low temperatures, with a smooth interpolation in between. The resulting critical temperature and the coexistence curve exponent are $\omega^* = 0.984$ (0.862 exact) and $\beta = 0.109$ (0.125 exact), again a significant improvement over MK ($\omega^* = 0.610$ and $\beta = 0.162$). Of course, the 2 × 2 cluster is merely the simplest example of a CDA calculation, but it is straightforward to extend these ideas to 2 × 4, 2 × 6, 4 × 4, and larger clusters. It is found that, as the cluster size increases, the calculated thermodynamic properties become more accurate. The thermodynamic functions can be obtained as outlined in Section 8 and Appendix A, where now the temperature-dependent $\lambda$ is used. As an example, Fig. 15 shows $\langle N_{AB}\rangle/N$ for the two-dimensional Ising model for the exact, 4 × 4 CDA, and MK calculations.

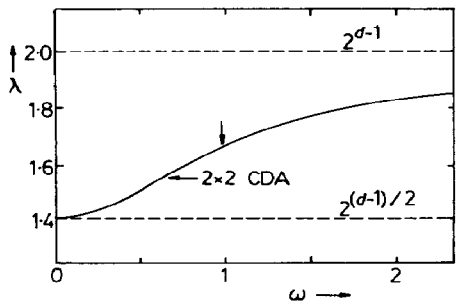


Fig. 14. Bond-strengthening parameter $\lambda$ for the two-dimensional Ising model using the 2 × 2 cluster of Fig. 13. The arrow indicates the critical coupling.

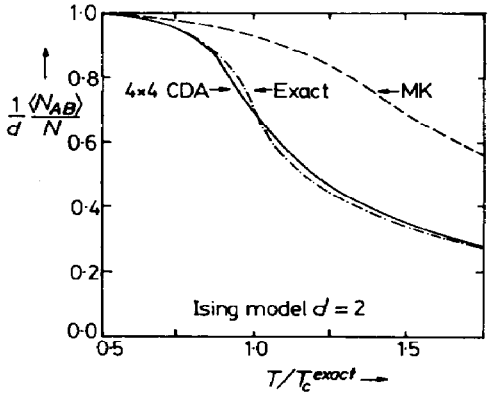


Fig. 15. Nearest-neighbor correlation for the two-dimensional Ising model. The horizontal axis is in units of the exact transition temperature.

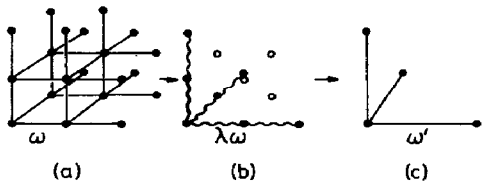


Fig. 16. Cluster-decimation approximation illustrated for the 2 × 2 × 2 cluster. Periodic boundary conditions are used here, just as for the 2 × 2 cluster.

The cluster-decimation method is almost equally easy to use in three dimensions. The appropriate 2 × 2 × 2 clusters are displayed in Fig. 16 and, as above, periodic boundary conditions are imposed. Now the cluster partition functions are

$$Z = 2e^{12\omega} + 16e^{6\omega} + 30e^{4\omega} + 48e^{2\omega} + 64 + 48e^{-2\omega} + 30e^{-4\omega} + 16e^{-6\omega} + 2e^{-12\omega}$$

and

$$Z_{\text{rst}} = 32e^{3\lambda\omega} + 96e^{\lambda\omega} + 96e^{-\lambda\omega} + 32e^{-3\lambda\omega}.$$

Though it is not possible to determine $\lambda$ analytically in this case, it is straightforward to obtain numerically the desired results on equating $Z$ and $Z_{\text{rst}}$. The results of this calculation are $\omega^* = 0.430$ (0.443 exact), $\beta = 0.440$ (0.3125 exact), again greatly improved over the simple MK ($\omega^* = 0.131$ and $\beta = 0.468$).

The benefits of the CDA method are particularly evident in the determination of thermodynamic functions. For example, Fig. 17 presents results for $\langle N_{AB}\rangle/N$, showing the clear superiority of the CDA over the MK calculations. Even more striking is the coexistence curve, which is displayed in Fig. 18. The "exact" results are obtained from Pade approximants to the most accurate series expansions known for the three-dimensional Ising model (Scesney, 1970). The MK result fails to even come close to the exact curve, although the CDA curve is satisfyingly accurate, es-

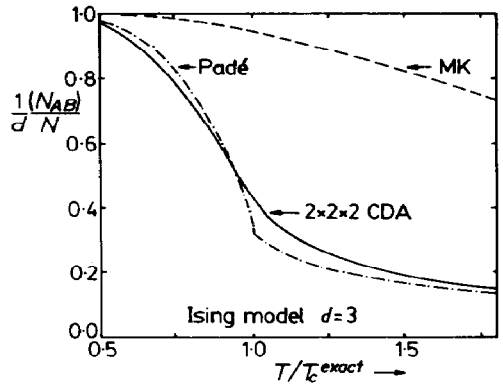


Fig. 17. Nearest-neighbor correlation for the three-dimensional Ising model. The horizontal axis is in units of the exact transition temperature.

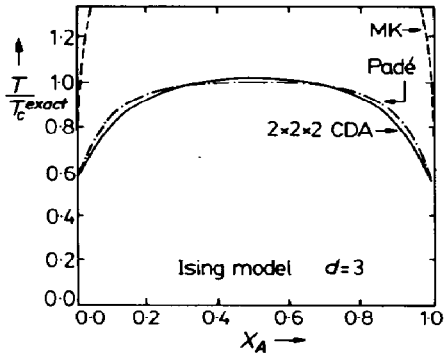


Fig. 18. Composition vs temperature for the three-dimensional Ising model. The Padé approximant results (exact) are from Scesney (1970), and the horizontal axis is in units of the exact transition temperature. The MK results fail badly, but the 2 × 2 × 2 cluster results, with no adjustable parameters, are in fairly good agreement.

pecially considering the simplicity of the calculation and the fact that no adjustable parameters are involved. It has been seen, then, that fairly simple modifications to the basic MK scheme can result in a quantitative computational method. Clearly, there is room for more work in these directions. For example, studies with nonzero $\Delta\tilde{\mu}$, and with more complex Hamiltonians, are still needed.

## 11. RECENT APPLICATIONS TO LIQUID MIXTURES

A specific example of RG theory as applied to solution thermodynamics (in particular, to systems which display complex miscibility phenomena) is now presented in detail. First, a brief discussion of the qualitative features of such systems is given, then a specific lattice model embodying these features is introduced. The model is studied using MK methods, as presented above, including some of the simple modifications, resulting in recursion relations which display a rather rich and complex structure of fixed points and RG flows. Physical meaning can be ascribed to each of the various fixed points, as well as to the precise nature of the flows. Finally, calculated phase diagrams are compared with experimental measurements.

The systems of interest are those binary liquid mixtures in which the miscibility behavior, instead of simply consisting of an upper critical solution point and phase separation at lower temperatures, is rather complex in that both upper and lower critical solution points (UCST and LCST, respectively) are observed. Thus, the two components are miscible in all proportions for temperatures above the UCST and below the LCST, whereas a miscibility gap exists between the two consolute points. (Examples are shown later in this section, in Figs 25–27.) Such behavior can be readily explained in terms of hydrogen bonding or other highly oriented attractive interactions between unlike components. The role of hydrogen bonds in producing complex miscibility phenomena was first pointed by Hirschfelder *et al.* (1937). Lattice models based on their ideas were introduced by Barker and Fock (1953), who studied them using a mean-field (quasichemical) approach. Decorated lattice versions were studied by Wheeler (1975) and Andersen and Wheeler (1978). The focus of this review will be on the most recently introduced lattice model for such mixtures, due to Walker and Vause (1980), which is well suited to RG analysis.

Consider a mixture in which the two types of molecules, $A$ and $B$, are capable of forming hydrogen bonds with one another. Bond formation is accompanied by a favorable energy change, but also by a great loss of orientational entropy, so that it can only occur at low temperatures. At higher temperatures, energetic effects are less important: all molecular orientations have equal probability. Since only a minuscule fraction of the randomly oriented molecules will be properly aligned to form bonds, the mixture behaves as if the bonding sites were not present at all. Nonoriented repulsions become dominant and cause the mixture to separate.

The Walker–Vause lattice model has three energy levels: (1) $AA$ and $BB$ pairs, with energies $\varepsilon_{AA}$ and $\varepsilon_{BB}$, which will be used to define the zero of energy; (2) $AB$ pairs with no hydrogen bond, represented by $A \cdot B$, with a positive energy $\varepsilon_{A \cdot B}$; and (3) $AB$ pairs with hydrogen bonding (denoted $A$–$B$) with a negative energy $\varepsilon_{A-B}$, the most favorable of the three. Hydrogen-bonded $A$–$A$ and $B$ $B$ pairs can be also considered (Goldstein and Walker, 1983) but such additional interactions will not be discussed here in the interest of clarity. Thus, only one additional parameter, $\varepsilon_{A-B}$, need be added to the Ising model to represent the energy of an $A$–$B$ bond.

The formation of a bond depends on the relative orientation of molecules $A$ and $B$. In the same spirit in which spatial positions are discretized in a lattice model, the orientation of a molecule is also taken to be in one of a finite, albeit rather large, number of directions. A discrete variable $\sigma = 1, 2 \ldots q$ is introduced to represent them. Since a hydrogen bond is highly oriented, it follows that $q$ will be a large

number; for the moment $q$ is left as an adjustable parameter. If an $A$ molecule occupies site $i$ and a $B$ molecule occupies site $j$, they will be regarded as forming a hydrogen bond if $\sigma_i = \sigma_j$. If, on the other hand, $\sigma_i \neq \sigma_j$, no bond can form. By analogy with eq. (9), two dimensionless exchange energies can be defined:

$$\omega_1 = (2\varepsilon_{A-B} - \varepsilon_{AA} - \varepsilon_{BB})/2kT < 0$$

and

$$\omega_2 = (2\varepsilon_{A\cdot B} - \varepsilon_{AA} - \varepsilon_{BB})/2kT > 0.$$

Since both $\sigma_i$ and $\sigma_j$ adopt the values $1, \ldots q$, it is clear that, of the total of $q^2$ possibilities, bonding occurs in $q$ ways and nonbonding occurs in $q(q-1)$ ways. The Hamiltonian of eq. (19) now becomes

$$\mathscr{H} = -N_{A-B}\omega_1 - N_{A\cdot B}\omega_2 + N_{AA}(2\Delta\tilde{\mu}/z) - N_{BB}(2\Delta\tilde{\mu}/z)$$

or, equivalently

$$\mathscr{H} = \sum_{nn} \mathscr{H}_{nn}$$

where the nearest-neighbor bond Hamiltonian, $\mathscr{H}_{nn}$, is displayed in Table 5. Note that Table 5 shows the features pointed out above. For example, the $A$–$B$ bonding interaction has the smallest degeneracy of any, by approximately a factor of $q$, and is unimportant at high temperatures.

For $\omega_1 = \omega_2 > 0$ the bonding energy is the same as that for nonbonding and, consequently, bonding does not exist. The model must then reduce to the simple Ising model (Table 4). This is verified by examining Table 5 in that limit. For $q = 1$ it is identical in all respects to the Ising model, while for $q > 1$ there is simply an additional $q$-fold degeneracy in all sites. The only effect of this is that $\ln q$ is added to the free energy per site, leaving the mixing properties unchanged. Thus, in the $\omega_1 = \omega_2 > 0$ "subspace" of the full $(\omega_1, \omega_2)$ space, the model should possess a simple UCST.

A MK calculation for the general model is now carried out, by analogy to the calculation presented above for the Ising model. An important difference is that all lengths will now be rescaled by a factor of three, in contrast to the factor of two used in the examples to this point. This change is made because $AB$ attractions ($\omega_1 < 0$) are of special importance in this problem, as illustrated in Fig. 19. In rescaling by a factor of two, a system that originally had a preponderance of $AB$ pairs will, after renormalization, be dominated by $AA$ and $BB$ pairs. However, when rescaling by a factor of three, the $AB$ pairs on the original lattice map onto $AB$ pairs after renormalization, thus preserving the character of the original system. A two-dimensional example of the bond-moving required for this transformation is shown in Fig. 20(a)–(c), where it is clear that the MK value of $\lambda$ is 3; of course the three-dimensional case is very similar, except then the bonds are strengthened by a factor of $\lambda = 9$. The previous study of the Ising model was confined to the case when the $AB$ interaction is repulsive. Thus, the $AA$ and $BB$ pairs dominate at low temperatures, and it is possible to rescale all lengths by a factor of two.

Having settled on bond-moving of the type displayed in Fig. 20, all that remains is to determine the corresponding recursion relations. As in the examples above, the next step is to sum over both decoupled and partially decoupled sites. Figure 20(c) shows the typical situation, where the sites on the ends are fully coupled while the intermediate sites are only partially

Table 5. Nearest-neighbor bond Hamiltonian, $\mathscr{H}_{nn}$, for the hydrogen-bonding mixture model

| $i-j$ | $\mathscr{H}_{nn}$ | Orientational degeneracy |
|---|---|---|
| $AA$ | $2\Delta\tilde{\mu}/z$ | $q^2$ |
| $A$–$B$ | $-\omega_1$ | $q$ |
| $A\cdot B$ | $-\omega_2$ | $q(q-1)$ |
| $BB$ | $-2\Delta\tilde{\mu}/z$ | $q^2$ |

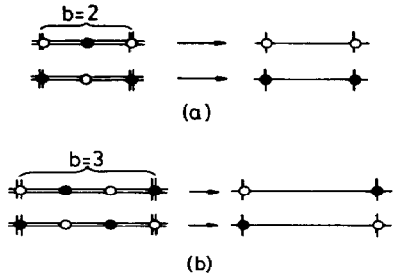


Fig. 19. Comparison of calculations in which lengths are rescaled by a factor of 2(a) or 3(b). When the rescaling is as in (a) a system with nearest neighbors that are predominantly $AB$ is mapped onto a system in which the nearest neighbors are $AA$ or $BB$. Rescaling by a factor of three ensures that the $AB$ character of the original system is preserved.

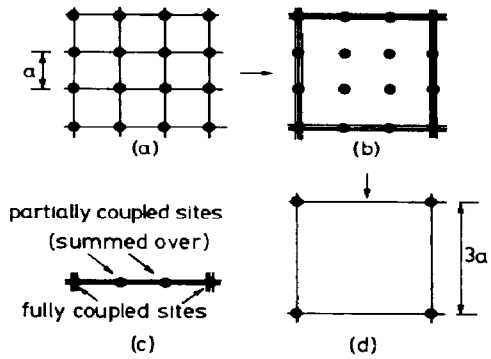


Fig. 20. Illustration of the steps involved in an MK calculation with lengths rescaled by a factor of 3. Shown here is a two-dimensional version of the actual three-dimensional calculation. First, certain bonds on the original lattice (a) are shifted to obtain a restructured lattice (b). On this lattice all partially coupled and decoupled molecules are summed over, resulting in lattice (d). The recursion relations are obtained by simply summing over the two intermediate molecules shown in (c).

coupled, and will be summed over. The recursion relations are generated by specifying the status of the end sites, and for each such specification summing over the intermediate sites. Note that the summation over the intermediate sites must now not only explore the identities of the molecules but also their orientations. In the Ising example of the previous sections there were three distinct specifications of the end sites, $AA$, $AB$ and $BB$. This yielded three recursion relations, from which the three renormalized quantities, $\omega'$, $\Delta\tilde{\mu}'$ and $g'$, were obtained. Now, there are four distinct specifications of the end sites $i$ and $j$, namely $AA$ and $BB$ (with arbitrary "orientations" $\sigma_i$ and $\sigma_j$), $A$–$B$ (for bonding "orientations" $\sigma_i = \sigma_j$) and $A \cdot B$ (for non-bonding "orientations" $\sigma_i \neq \sigma_j$). Any other choice for the states of the two end sites simply gives the same information as in one of the above specifications. These four cases will result in four recursion relations which can be used to determine the four renormalized parameters $\omega_1'$, $\omega_2'$, $\Delta\tilde{\mu}'$ and $g'$.

The recursion relations for this model for hydrogen-bonding mixtures are derived in detail in the literature (Walker and Vause, 1983); for the sake of brevity they will not be rederived here. However, it should be pointed out that, as with the simple Ising model, these equations enjoy the following useful property: when $\Delta\tilde{\mu} = 0$ then $\Delta\tilde{\mu} = 0$ also. Thus $\Delta\tilde{\mu} = 0$ is what is known as an "invariant" subspace. Furthermore, by symmetry, this is the region in which the phase coexistence surface lies. The discussion will be limited to this subspace, in which case the recursion relations are

$$\omega_1' = \ln(z_0/z_1)$$
$$\omega_2' = \ln(z_0/z_2)$$

where

$$z_0 = q^2 + 3x^2 + 6(q-1)xy + 3(q-1)^2y^2$$
$$z_1 = x^3 + 3(q-1)xy^2 + (q-1)(q-2)y^3 + 3qx + 3q(q-1)y$$
$$z_2 = 3x^2y + 3(q-2)xy^2 + (q^2-3q-3)y^3 + 3qx + 3q(q-1)y$$

and $x = \exp(-\lambda\omega_1)$, $y = \exp(-\lambda\omega_2)$. In a MK calculation with no modification $\lambda = 3^{d-1}$ for the bond-moving used here, i.e. $\lambda = 9$ in three dimensions. We shall take $\lambda$ to be a free parameter in order to improve the accuracy of the MK calculation, as described in the previous section.

The $(\omega_1, \omega_2)$ plane is plotted in Fig. 21. Note that the $(\omega_1, \omega_2)$ space divides into three regions, labeled I, II and III. The meaning of these regions, in terms of the RG transformation, is that all flows within a given region approach the same fixed point. For example, if the initial values of $\omega_1$ and $\omega_2$ correspond to the point $a_1$ in Fig. 21, then after one iteration of the recursion relations $\omega_1'$ and $\omega_2'$ corresponding to the point $a_2$ are obtained. A further iteration renormalizes $\omega_1'$ and $\omega_2'$ to the point indicated by $a_3$, and so on. The points

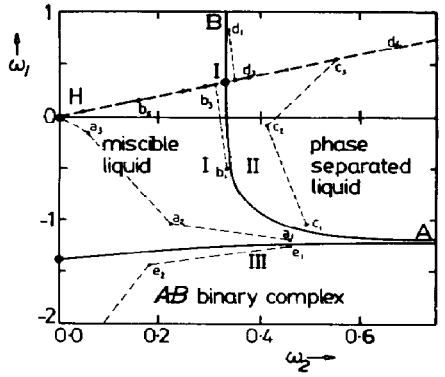


Fig. 21. Phase diagram in $(\omega_1, \omega_2)$ space. Three distinct phases are represented: miscible liquid (I), phase-separated liquid (II), and $A$–$B$ binary complex (III). The solid lines indicate the phase transition between these phases. Examples of renormalization group flows are indicated by numbered sets of points, such as $a_1', a_2, \ldots$. The dashed line is the invariant Ising subspace.

$a_1, a_2, a_3 \ldots$ are the RG flow associated with the initial point $a_1$. It is clear from the figure that this flow approaches the fixed point at the origin, labeled **H**, as does the flow starting at the point $b$. Every point in region I, by definition, flows to the fixed point **H** as the RG is iterated. Similarly, every point in region II flows to the fixed point **L**, which is located at $\omega_1 = \omega_2 \to \infty$. Several examples are shown. Finally, points in region III flow to the fixed point **C**, $\omega_1 \to -\infty$, $\omega_2 = 0$, as illustrated in Fig. 21.

As in the earlier analysis of the simple Ising model, the significance of the three regions defined by the RG transformation lies in the fact that the recursion relations are analytic. This means, for example, that a system at point $a_1$ (i.e. with $\omega_1$ and $\omega_2$ corresponding to $a_1$) is related by a series of analytic transformations to the point **H**. Therefore, $a_1$ and **H** are in the same thermodynamic phase of the model since a system can go from one phase to another only by passing through a nonanalytic singularity or a discontinuity, i.e. it must pass through a phase transition. Thus, each of the three regions corresponds to a distinct thermodynamic phase of the system, and the boundaries separating these regions correspond to the phase transitions.

The physical characteristics of each region can be obtained by considering the fixed point which defines, or governs, that region. These fixed points, such as **H**, **L** and **C**, are phase sinks, since all flows in a given type of phase converge on them. Each sink represents the extreme example of that particular phase. Thus, for example, the fixed point **H** is at $\omega_1 = \omega_2 = 0$, i.e. all the interactions are zero. This is the extreme case of high temperature (**H**), and thus the system is completely random, and hence miscible. Region I can then be identified as the region of complete miscibility. At point **L**, $\omega_1 = \omega_2 \to \infty$, the couplings are infinitely strong, corresponding to the extreme of low temperature (**L**), and so here the system is perfectly phase

separated. Clearly, region II contains all immiscible mixtures. Finally, at sink **C** the system is again at low temperatures, since the coupling is infinitely large, but now instead of being phase-separated it exists as an $A$–$B$ binary complex.

The line **AIB** is the boundary between regions I and II, belonging to neither. Consequently, a flow beginning on **AIB** must always remain there. The line **AIB** is a one-dimensional region, all points of which flow to the fixed point **I**, and share its properties. To see the meaning of this fixed point, first recall that when $\omega_1 = \omega_2$ the bonding model reduces to the simple Ising model. Recall also that $\Delta\tilde{\mu} = 0$; thus the dashed line corresponds to the $\Delta\tilde{\mu} = 0$ axis in Fig. 9. Clearly, **I** is the Ising critical point, corresponding to the critical solution temperature. As such, all points on **AIB** are also Ising critical solution points. The line $\omega_1 = \omega_2$ will be referred to as the Ising subspace. It can be shown that it is an invariant subspace, i.e. $\omega_1 = \omega_2$ implies that $\omega_1' = \omega_2'$.

To relate the present model to a specific mixture, it is useful to consider the ratio $R \equiv \omega_1/\omega_2$. This quantity is temperature-dependent, being simply the ratio of the bonding to nonbonding energies. Thus a given binary mixture is characterized by its value of $R$, and the initial point representing the mixture moves along a straight line through the origin as the temperature varies, moving closer to the origin as the temperature increases. As a first example, consider a mixture that does not bond at all, that is $R = 1$. This is just the simple binary (Ising) case, with properties that are well understood. As noted above, at the lowest temperature (point **L**) the mixture is perfectly phase-separated. Moving along the line **LIH**, the temperature increases until, at the critical solution point **I**, the two phases become identical. At even higher temperatures, from **I** to **H**, the system is in the region of complete miscibility.

Turning now to bonding systems, Fig. 22 shows four examples, each characterized by a value of $R$ and indicated by a dashed line. Line 1 corresponds to a mixture for which the "bonding" energy is still repulsive ($\omega_1 > 0$) but less so than the nonbonding energy. The behavior is qualitatively similar to that of a nonbonding mixture. Line 2 describes the case of $\omega_2 < 0$, when the directed $A$–$B$ interaction is attractive, i.e. bonding. In this case the system is miscible from **H** to **Up**, at which point it becomes critical: this is the upper critical solution temperature. For lower temperatures, from **Up** to **Lo**, the system is immiscible (with flows terminating at **L**) but again becoming critical at **Lo**, the lower critical solution temperature. As the system is cooled through the point **Lo** it again enters the miscible phase, the flows now being attracted to **H**. As the bonding energy becomes stronger, i.e. as $\omega_1$ becomes more negative, the temperature range of immiscibility decreases. Line 3 shows the limiting case when the upper and lower critical solution points merge in a mixture at incipient separation. For even more attractive bond strengths, as in line 4, the mixture remains miscible at all temperatures.

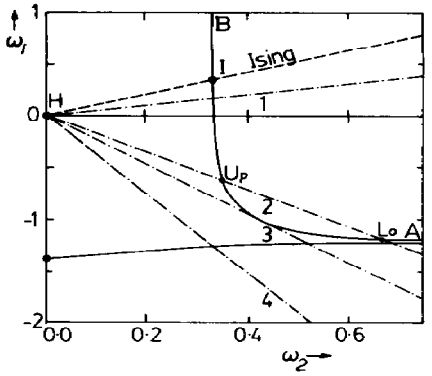


Fig. 22. Types of behavior expected for various values of $\omega_1/\omega_2$. In case 1 the bonding energy is repulsive ($\omega_1 > 0$) so that, as the temperature is lowered, i.e. as one moves away from the origin, only a single critical point is encountered. Cases 2–4 correspond to favorable bonding energies ($\omega_1 < 0$). For moderately strong bonds the system may display an upper and a lower critical point, as in 2, or these points may coalesce as in 3. If the bonds are too strong the system may not phase separate at all, as in 4, but, rather, remain miscible until freezing occurs.

Since it is now clear that close-loop phase diagrams result from this calculation, it remains to obtain the composition $x_A$ so that quantitative results may be presented. The procedures outlined in Appendix A for calculating thermodynamic quantities are followed for the case of interest here, namely, $\Delta\tilde{\mu} = 0$. The composition iterates under the RG as

$$(2x_A - 1) = \frac{1}{8}\left(\frac{\partial\Delta\tilde{\mu}'}{\partial\Delta\tilde{\mu}}\right)_{\omega_1,\omega_2}\Bigg|_{\Delta\tilde{\mu}=0}(2x_A - 1)'.$$

Evaluating the derivative for the present case results in the more explicit result

$$(2x_A - 1) = \left(\frac{8q^2 + z_0}{9z_0}\right)(2x_A - 1)'.$$

This relation is iterated until the flow approaches either **H** or **L** sufficiently close for convergence to occur. Thus

$$(2x_A - 1) = \left(\frac{8q^2 + z_0}{9z_0}\right)\left(\frac{8q^2 + z_0}{9z_0}\right)'(2x_A - 1)''$$
$$= P^{\infty}(2x_a - 1)^{(\infty)}$$

where

$$P^{\infty} = \prod_{n=0}^{\infty}\left(\frac{8q^2 + z_0}{9z_0}\right)^{(n)}$$

and $P^{(0)} = 1$. Convergence is attained when the value of the continued product stabilizes to within a desired tolerance, which typically occurs for $n \leqslant 10$. At the fixed points the value of $(2x_A - 1)$ [i.e. $(2x_a - 1)^{(\infty)}$] is known; that is, at infinite temperature $x_{A,\mathbf{H}} = 0.5$, while at zero temperature it is clear that $x_{A,\mathbf{L}} = 1.0$. Table 6 presents examples of flows, along with the corresponding convergence of the calculated composition.

Table 6. Examples of MK flows, showing convergence of the continued product $P^{(n)}$ which is directly related to the composition†

| $n$ | $\omega_1$ | $\omega_2$ | $P^{(n)}$ |
|---|---|---|---|
| 0 | −1.000 | 0.450 | 1.000 |
| 1 | 0.084 | 0.386 | 0.841 |
| 2 | 0.478 | 0.478 | 0.733 |
| 3 | 0.758 | 0.758 | 0.682 |
| 4 | 1.744 | 1.744 | 0.676 |
| 5 | 5.418 | 5.418 | 0.676 |

(a)

| $n$ | $\omega_1$ | $\omega_2$ | $P^{(n)}$ |
|---|---|---|---|
| 0 | −1.000 | 0.350 | 1.000 |
| 1 | −0.014 | 0.219 | 0.757 |
| 2 | 0.116 | 0.116 | 0.508 |
| 3 | 0.019 | 0.019 | 0.256 |
| 4 | 0.000 | 0.000 | 0.092 |
| 5 | 0.000 | 0.000 | 0.031 |
| 6 | 0.000 | 0.000 | 0.010 |
| 7 | 0.000 | 0.000 | 0.003 |
| 8 | 0.000 | 0.000 | 0.001 |
| 9 | 0.000 | 0.000 | 0.000 |

(b)

| $n$ | $\omega_1$ | $\omega_2$ | $P^{(n)}$ |
|---|---|---|---|
| 0 | −0.500 | 1.000 | 1.000 |
| 1 | 2.199 | 2.209 | 0.996 |
| 2 | 7.157 | 7.157 | 0.996 |

(c)

| $n$ | $\omega_1$ | $\omega_2$ | $P^{(n)}$ |
|---|---|---|---|
| 0 | −0.500 | 0.339 | 1.000 |
| 1 | 0.326 | 0.328 | 0.817 |
| 2 | 0.328 | 0.328 | 0.667 |
| 3 | 0.328 | 0.328 | 0.545 |
| 4 | 0.328 | 0.328 | 0.446 |
| 5 | 0.329 | 0.329 | 0.364 |
| 6 | 0.332 | 0.332 | 0.298 |
| 7 | 0.338 | 0.338 | 0.245 |
| 8 | 0.354 | 0.354 | 0.203 |
| 9 | 0.394 | 0.394 | 0.171 |
| 10 | 0.502 | 0.502 | 0.151 |
| 11 | 0.839 | 0.839 | 0.142 |
| 12 | 2.041 | 2.041 | 0.141 |
| 13 | 6.530 | 6.530 | 0.141 |

(d)

† Iterations are indexed by $n$, so that $n = 0$ corresponds to the initial point $(\omega_1, \omega_2)$, $n = 1$ refers to $(\omega_1', \omega_2')$, and so on. Notice that the flows converge quickly onto the Ising subspace, $\omega_1 = \omega_2$. Flow (a) goes to the sink $\mathbf{L}(\omega_1 = \omega_2 = \infty)$, in which case $(2x_A - 1)^\infty = 1$; thus, one can obtain $x_A$ for the initial point through the relation $(2x_A - 1) = P^{(\infty)}(2x_A - 1)^{(\infty)}$. Case (b) flows to the sink $\mathbf{H}$, and clearly $x_A = 0.5$. Case (c) illustrates an initial point far from the phase transition; note the very rapid convergence. In contrast, case (d) is quite close to the phase boundary and thus requires more iterations for convergence.

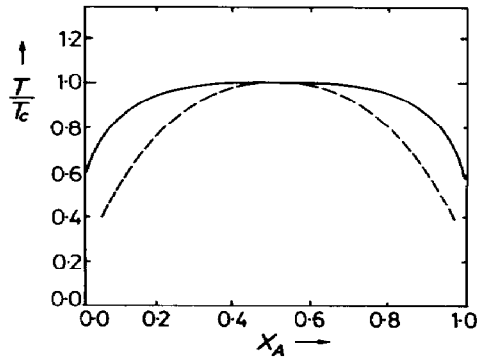


Fig. 23. Comparison of compositions from exact and MK calculations for $\omega_1 = \omega_2$. The exact result for the composition (Scesney) is shown by the solid line. The standard MK calculation, with $\lambda = 9$, yields the results given by the dashed line. By adjusting the parameter $\lambda$ the MK calculation can be improved to the extent that for $\lambda = 3.74$ the approximate and exact results are indistinguishable on this scale. This same value of $\lambda$ will be used for calculations when $\omega_1 \neq \omega_2$.

In order to compare with experiment it is necessary to improve the MK calculation so that quantitatively accurate results may be obtained. The results for the Ising model are first considered as these can be compared with exact calculations. Figure 23 shows the composition calculated for $R = 1$, compared with the exact curve (Scesney, 1970). As in the previous section, the bond-strengthening parameter $\lambda$ is adjusted, using the criterion that the calculated composition be in close agreement with the exact values. It is found that for $\lambda = 3.74$ the calculation is indistinguishable from the exact, on the scale of Fig. 23. For this $\lambda$, it is also found that $\beta = 0.23$, while to obtain the accepted value for $\beta$, namely 0.32, $\lambda$ must equal 5.8. However, since the overall phase diagram is of primary interest here, $\lambda$ is chosen as 3.74. Figure 24 compares data for glycerol + methyl ethyl ketone with the modified MK calculation for $R = 1$.

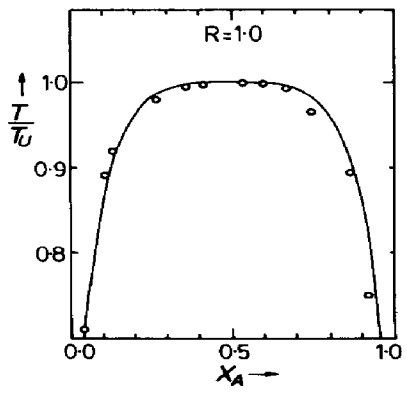


Fig. 24. Temperature–composition phase diagram for glycerol + methyl ethyl ketone. The points represent data, while the solid curve is the MK result, calculated with $\omega_1 = \omega_2$. The fluid is miscible outside the curve, and consists of two coexisting phases within it.

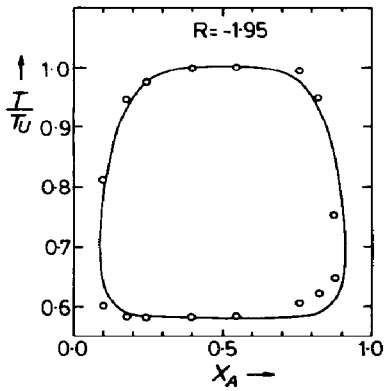


Fig. 25. Temperature–composition phase diagram for glycerol + benzylethylamine. The points represent data, while the solid curve is the MK result, calculated with $\omega_1/\omega_2 = -1.95$.

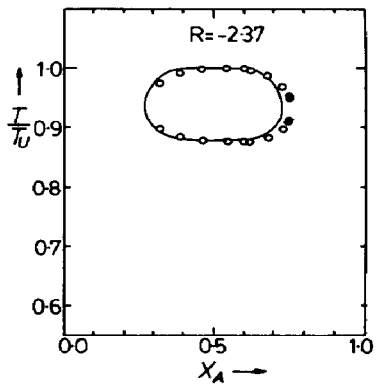


Fig. 27. Temperature–composition phase diagram for glycerol + guaiacol. The points represent data, while the solid curve is the MK result, calculated with $\omega_1/\omega_2 = -2.37$.

Without changing the bond-strengthening factor $\lambda$, predictions for hydrogen-bonding systems can be examined. First, in Fig. 25, data for glycerol + benzylethylamine are compared to the results of the calculations for $R = -1.95$. There are two parameters involved in this fit, corresponding to the two characteristics of the hydrogen bond. $R = \omega_1/\omega_2$ measures the relative strength of bonding, while $q$ is a measure of the entropy lost in forming a bond. The main effect of $q$ is to vary the width of the closed loops, and it is by this criterion that $q = 500$ is obtained. It should be noted that $q = 500$ (corresponding to dividing the total solid angle into 500 pieces) implies an angular width for bonding of roughly 10°, in accord with the usual picture of hydrogen bonds (Vinogradov and Linnell, 1971). The agreement with experiment is quite satisfactory in all respects.

Figures 26 and 27 show two more examples of closed loops in glycerol mixtures. In each case $q = 500$ is used, since the directionality associated with the hydrogen bonds would not be expected to differ greatly in going from one of these systems to another. However, the strength of the bonding may certainly be different, and good fits to the data are obtained with the values of $R$ indicated in Fig. 26 and 27.

Finally, it is found that the bonding in the case of guaiacol is so strong that phase separation has almost entirely disappeared. In fact, more recent experiments indicate that the original measurements, shown here, probably contained approximately 2.8% water, due to the affinity for water displayed by guaiacol. The water competes for hydrogen-bonding sites, thus lessening the effective glycerol–guaiacol bonding strength. If care is taken to remove the water the full bonding strength of the guaiacol is realized, and the loop vanishes. This ability to change the size of the loop, and indeed to cause its disappearance if desired, has recently been exploited to study interesting behavior just at the point of vanishing (Johnson *et al.*, 1985).

An example has been given here of a rather interesting class of binary mixtures, which can be well described by a simple lattice model. A MK calculation reveals the existence of closed-loop phase diagrams, and points up methods for interpreting fixed points and flows. A simple modification of the usual MK transformation allows for quantitative comparison with experiments. As time progresses, it is certain that more and more systems of interest in solution thermodynamics will be analyzed and better understood with the aid of such renormalization group techniques.

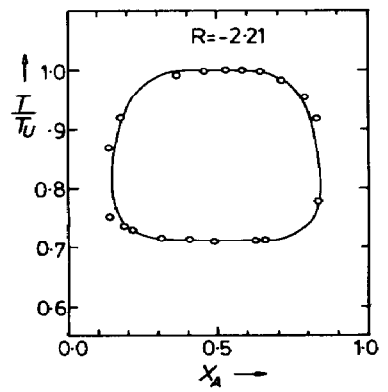


Fig. 26. Temperature–composition phase diagram for glycerol + *m*-toluidine. The points represent data, while the solid curve is the MK result, calculated with $\omega_1/\omega_2 = -2.21$.

## NOTATION

| | |
|---|---|
| $b$ | renormalization group scale factor |
| $E$ | internal energy |
| $E_i$ | energy of configuration $i$ |
| $g$ | bond normalization factor |
| $\mathscr{H}$ | dimensionless Hamiltonian |
| $\mathscr{H}_{nn}$ | dimensionless bond Hamiltonian |
| $k$ | Boltzmann constant |
| $K$ | dimensionless normalization parameter |
| $N$ | total number of particles |
| $N_i$ | number of particles of species $i$ |
| $N_{ij}$ | number of nearest-neighbor $ij$ interactions |
| $P$ | pressure |

$P$ renormalization group projection function
$q$ orientational degrees of freedom parameter
$S$ entropy
$T$ temperature
$V$ volume
$v$ dimensionless Hamiltonian perturbation
$x$ mole fraction
$\underline{x}$ lattice configurational state
$Y$ semigrand Massieu potential
$z$ lattice coordination number
$z$ particle configurational free energy
$Z$ configurational partition function
$Z_{rst}$ restructured lattice configurational partition function
$Z'$ renormalized lattice configurational partition function

$\alpha$ specific heat critical exponent
$\beta$ coexistence curve critical exponent
$\varepsilon_{ij}$ $ij$ interaction energy
$\lambda$ bond strengthening factor
$\mu_i$ chemical potential of species $i$
$\Delta\tilde{\mu}$ dimensionless chemical potential difference
$\nu$ correlation length critical exponent
$\xi$ correlation length
$\sigma$ bond orientational state
$\Psi$ semigrand canonical partition function
$\omega$ dimensionless exchange energy

## REFERENCES


Abrams, D. S. and Prausnitz, J. M., 1975, A new expression for the excess Gibbs energy of partly or completely miscible systems. *A.I.Ch.E. J.* **21**, 116–128.

Amit, D., 1984, *Field Theory, the Renormalization Group and Critical Phenomena*. World Scientific, Singapore.

Andelman, D. and Walker, J. S., 1983, Preserving the free energy in a Migdal–Kadanoff approximation for the $q$-state Potts model. *Phys. Rev. B* **27**, 241–247.

Andersen, G. R. and Wheeler, J. C., 1978, Theory of lower critical solution points in aqueous mixtures. *J. chem. Phys.* **69**, 3403–3413.

Barber, M. N., 1977, Introduction to the fundamentals of the renormalization group in critical phenomena. *Phys. Rep.* **29**, 1–84.

Barker, J. A., 1952, Cooperative orientational effects in solutions. *J. chem. Phys.* **20**, 1526–1532.

Barker, J. A., 1963, *Lattice Theories of the Liquid State*. Macmillan, New York.

Barker, J. A. and Fock, W., 1953, Theory of upper and lower critical solution temperatures. *Discuss. Faraday Soc.* **15**, 188–195.

Binder, K. (Ed.), 1979, *Monte Carlo Methods*, Topics in Current Physics Vol. 7, 2nd edition. Springer, Berlin.

Binder, K. (Ed.), 1983, *Monte Carlo Methods: Applications in Statistical Physics*, Topics in Current Physics Vol. 36. Springer, Berlin.

Brezin, E., LeGuillon, J. C. and Zinn-Justin, J., 1976, Field theoretical approach to critical phenomena. In *Phase Transitions and Critical Phenomena* (Edited by C. Domb and M. S. Green), Vol. 6, pp. 125–247. Academic Press, New York.

Brush, S. G., 1967, History of the Lenz–Ising model. *Rev. mod. Phys.* **39**, 883–893.

Burkhardt, T. W. and Leeuwen, J. M. J. van (Eds), 1982, *Real-space Renormalization*, Topics in Current Physics Vol. 30. Springer, Berlin.

Callen, H. B., 1985, *Thermodynamics and an Introduction to Thermostatistics*, 2nd edition. Wiley, New York.

Caracciolo, S., 1981, Improved Migdal recursion formulae for the Ising model in two dimensions on a triangular lattice. *Nucl. Phys.* **B180**, 405–416.

Carnahan, N. F. and Starling, K. E., 1969, Equation of state for nonattracting rigid spheres. *J. chem. Phys.* **51**, 635–636.

Domb, C., 1974, Ising model. In *Phase Transitions and Critical Phenomena* (Edited by C. Domb and M. S. Green), Vol. 3, pp. 357–484. Academic Press, New York.

Domb, C., 1981, Critical phenomena—a model illustration of scientific method. In *Perspectives in Statistical Physics* (Edited by H. J. Raveche), pp. 173–200. North-Holland, Amsterdam.

Domb, C. and Green, M. S. (Eds), 1972–1986, *Phase Transitions and Critical Phenomena*, Vols 1–9. Academic Press, New York.

Eckert, C. A., Thomas, E. R. and Johnston, K. P., 1980, Nonelectrolyte solutions; state of the art review. In *Phase Equilibria and Fluid Properties in the Chemical Industry Proc.* (*Part* II), EFCE Pub. Ser. 11, pp. 399–417. Dechema, Berlin.

Fisher, M. E., 1964, Correlation functions and the critical region of simple fluids. *J. math. Phys.* **5**, 944 962.

Fisher, M. E., 1983, Scaling, universality and renormalization group theory. In *Critical Phenomenea*, Lecture Notes in Physics 186 (Edited by F. J. W. Hahne), pp. 1–139. Springer, Berlin.

Fox, J. R., 1983, Method for construction of non-classical equations of state. *Fluid Phase Equilibria* **14**, 45–53.

Freed, K. F., 1987, *Renormalization Group Theory of Macromolecules*. Wiley, New York.

Gennes, P. G. de, 1979, *Scaling Concepts in Polymer Physics*. Cornell University Press, Ithaca, NY.

Goldstein, R. E. and Walker, J. S., 1983, Theory of multiple phase separations in binary mixtures. *J. chem. Phys.* **78**, 1492–1512.

Goldstein, R. E. and Walker, J. S., 1985, Thermodynamic functions and critical properties from a cluster-decimation approximation. *J. Phys. A* **18**, 1275–1287.

Gray, C. G. and Gubbins, K. E., 1984, *Theory of Molecular Fluids*, Vol. 1. Clarendon Press, Oxford.

Guggenheim, E. A., 1952, *Mixtures*. Clarendon Press, Oxford.

Gunton, J. D. and Droz, M., 1983, *Introduction to the Theory of Metastable and Unstable States*. Springer, Berlin.

Haile, J. M., 1986, Computer simulation of fluid mixtures. *Fluid Phase Equilibria* **29**, 307–325.

Henderson, D., 1978, Practical calculations of the equations of state of fluids and fluid mixtures using perturbation theory and related theories. In *Equations of State in Engineering and Research*, Advances in Chemistry 182, pp. 1–30. American Chemical Society, Washington, DC.

Hill, T. L., 1956, *Statistical Mechanics*. McGraw-Hill, New York.

Hirschfelder, J., Stevenson, D. and Eyring, H., 1937, A theory of liquid structure. *J. chem. Phys.* **5**, 896–912.

Hoover, W. G., Alder, B. J. and Ree, F. H., 1964, Dependence of lattice gas properties on mesh size. *J. chem. Phys.* **41**, 3528–3533.

Hsu, S. C., Neimeijer, Th. and Gunton, J. D., 1975, Improved cumulant expansion for a renormalization group treatment of Ising models. *Phys. Rev. B* **11**, 2699–2701.

Hu, B., 1982, Introduction real-space renormalization-group methods in critical and chaotic phenomena. *Phys. Rep.* **91**, 233–295.

Hu, C.-K., Chen, W.-D., Shih, Y.-M., Jou, D.-C., Pan, C. K., Huang, H. M., Chen, K.-G., Lee, W. S., Wan, D. S. and Tseng, H.-C., 1981, Lower bound approximation to the free energy of an Ising model on a simple cubic lattice. *Can. J. Phys.* **59**, 1291–1295.

Huang, K., 1987, *Statistical Mechanics*, 2nd edition. Wiley, New York.

Johnson, R. G., Clark, N. A., Wittzius, P. and Cannell, D. S., 1985, Critical behavior near a vanishing miscibility gap. *Phys. Rev. Lett.* **54**, 49–52.

Jose, J. V., Kadanoff, L. P., Kirkpatrick, S. and Nelson, D. R., 1977, Renormalization vortices and symmetry breaking perturbations in 2-D planar models. *Phys. Rev. B* **16**, 1217–1241; Erratum, *ibid.* **17**, 1477.

Kadanoff, L. P., 1966, Scaling laws for Ising models near Tc. *Physics* **2**, 263–272.

Kadanoff, L. P., 1975, Variational principles and approximate renormalization group calculations. *Phys. Rev. Lett.* **34**, 1005–1008.

Kadanoff, L. P., 1976a, Scaling universality and operator algebras. In *Phase Transitions and Critical Phenomena* (Edited by C. Domb and M. S. Green), Vol. 5a, pp. 1–34. Academic Press, New York.

Kadanoff, L. P., 1976b, Notes on Migdal's recursion formulas. *Ann. Phys.* **100**, 359–394.

Kadanoff, L. P. and Houghton, A., 1975, Numerical evolution of the critical properties of the two-dimensional Ising model. *Phys. Rev. B* **11**, 377–386.

Kadanoff, L. P., Houghton, A. and Yalabik, M. C., 1976, Variational approximation for renormalization group transformation. *J. statist. Phys.* **14**, 171–203.

Kleintjens, L. A., 1985, Mean-field lattice gas description of vapor–liquid and supercritical equilibrium. *Fluid Phase Equilibria* **10**, 183–190.

Kumar, A., Krishnamurthy, H. R. and Gopal, E. S. R., 1983, Equilibrium critical phenomena in binary liquid mixtures. *Phys. Rep.* **98**, 57–143.

Lancombe, R. H. and Sanchez, I. C., 1976, Statistical thermodynamics of fluid mixtures. *J. phys. Chem.* **80**, 2568–2580.

Leeuwen, J. M. J. van, 1975, Renormalization theory for spin systems. In *Fundamental Problems in Statistical Mechanics* (Edited by E. G. D. Cohen), pp. 81–101. North-Holland, Amsterdam.

Levelt Sengers, J. M. H. and Sengers, J. V., 1975, Universality of critical behavior in gases. *Phys. Rev. A* **12**, 2622–2627.

Levelt Sengers, J. M. H. and Sengers, J. V., 1981, How close is "close to the critical point"? In *Perspectives in Statistical Physics* (Edited by H. J. Raveche), pp. 239–271. North-Holland, Amsterdam.

Lewis, G. N. and Randall, M., 1961, *Thermodynamics*, 2nd edition. Revised by K. S. Pitzer and L. Brewer. McGraw-Hill, New York.

Ma, S. K., 1976, *Modern Theory of Critical Phenomena*. Benjamin, New York.

Maitland, G. C., Rigby, M., Smith, E. B. and Wakeham, W. A., 1981, *Intermolecular Forces*, Clarendon Press, Oxford.

Maris, H. J. and Kadanoff, L. P., 1978, Teaching the renormalization group. *Am. J. Phys.* **46**, 652–657.

Mazenko, G. F. and Valls, O. T., 1982, The real-space dynamic renormalization group. In *Real-space Renormalization*, Topics in Current Physics Vol. 30 (Edited by T. W. Burkhardt and J. M. J. van Leeuwen), pp. 87–117. Springer, Berlin.

McHugh, M. A. and Krukonis, V. J., 1986, *Supercritical Fluid Extraction*. Butterworths, Stoneham, MA.

Migdal, A. A., 1976, Phase transformations in gauge and spin-lattice systems. *Soviet Phys. JETP* **42**, 743–746.

Modell, M. and Reid, R. C., 1983, *Thermodynamics and Its Applications*, 2nd edition. Prentice-Hall, Englewood Cliffs, NJ.

Moldover, M. R. and Gallagher, J. S., 1978, Critical points of mixtures: an analogy with pure fields. *A.I.Ch.E. J.* **24**, 267–278.

Münster, A., 1966, Critical fluctuations. In *Fluctuation Phenomena in Solids* (Edited by R. E. Burgess), pp. 179–266. Academic Press, New York.

Münster, A., 1969, *Statistical Thermodynamics*, Vol. 1. Springer, Berlin.

Nauenberg, M. and Nienhuis, B., 1974a, Critical surface for square Ising spin models. *Phys. Rev. Lett.* **33**, 944–946.

Nauenberg, M. and Nienhuis, B., 1974b, Renormalization-group approach to the solution of general Ising models. *Phys. Rev. Lett.* **33**, 1598–1601.

Neimeijer, Th. and Leeuwen, J. M. J. van, 1973, Wilson theory for spin systems on a triangular lattice. *Phys. Rev. Lett.* **31**, 1411–1414.

Neimeijer, Th. and Leeuwen, J. M. J. van, 1974, Wilson theory for 2-dimensional Ising spin systems. *Physica* **71**, 17–40.

Neimeijer, Th. and Leeuwen, J. M. J. van, 1976, Renormalization theory for Ising-like spin systems. In *Phase Transitions and Critical Phenomena* (Edited by C. Domb and M. S. Green), Vol. 6, pp. 425–505. Academic Press, New York.

Nightingale, M. P., 1976, Scaling theory and finite systems. *Physica* **83A**, 561–572.

Onsager, L., 1944, Crystal statistics. *Phys. Rev.* **65**, 117–149.

Oono, Y., 1985, Statistical physics of polymer solutions: conformation-space renormalization-group approach. *Adv. chem. Phys.* **61**, 301–437.

Panayiotou, C. and Vera, J. H., 1980, The quasi-chemical approach for non-randomness in liquid mixtures. *Fluid Phase Equilibria* **5**, 55–80.

Paulaitis, M. E., Penninger, J. M. L., Gray, R. D., Jr. and Davidson, P. (Eds), 1983, *Chemical Engineering at Supercritical Fluid Conditions*. Ann Arbor Science, Ann Arbor, MI.

Penninger, J. M. L., Radosz, M., McHugh, M. A. and Krukonis, V. J. (Eds), 1985, *Supercritical Fluid Technology*. Elsevier, Amsterdam.

Peng, D. Y. and Robinson, D. B., 1976, A new two constant equation of state. *Ind. Engng Chem. Fundam.* **15**, 59–64.

Pfeuty, P. and Toulouse, G., 1977, *Introduction to the Renormalization Group and to Critical Phenomena*. Wiley, New York.

Prausnitz, J. M., Lichtenthaler, R. N. and Azevedo, E. G., 1986, *Molecular Thermodynamics of Fluid-phase Equilibria*, 2nd edition. Prentice-Hall, Englewood Cliffs, NJ.

Quirke, N., 1986, Molecular simulation: progress and prospects. *Fluid Phase Equilibria* **29**, 283–306.

Redlich, O. and Kwong, J. N. S., 1949, On the thermodynamics of solutions. *Chem. Rev.* **44**, 233–244.

Rowlinson, J. S. and Swinton, F. L., 1982, *Liquids and Liquid Mixtures*, 3rd edition. Butterworths, London.

Schick, M., 1982, Applications of the real-space renormalization to adsorption systems, In *Real-space Renormalization*, Topics in Current Physics Vol. 30 (Edited by T. W. Burkhardt and J. M. J. van Leeuwen), pp. 149–168. Springer, Berlin.

Smith, W. R., 1973, Perturbation theory in classical statistical mechanics of fluids. In *Statistical Mechanics*, Vol. 1, pp. 71–133. Specialist Periodical Report, Chemical Society, London.

Squires, T. G. and Paulaitis, M. E. (Eds), 1987, *Supercritical Fluids*, ACS Symp. Series 329. American Chemical Society, Washington.

Stanley, H. E., 1971, *Phase Transitions and Critical Phenomena*. Oxford University Press, New York.

Stanley, H. E., 1981, New directions in percolation, In *Disordered Systems and Localization*, Lecture Notes in Physics 149, pp. 59–83. Springer, Berlin.

Stanley, H. E., Reynolds, P. J., Redner, S. and Family, F., 1982, Position-space renormalization group methods for models of linear polymers, branched polymers and gels, In *Real-space Renormalization*, Topics in Current Physics Vol. 30 (Edited by T. W. Burkhardt and J. M. J. van Leeuwen), pp. 169–206. Springer, Berlin.

Subbarao, K., 1975, Renormalization group for Ising spins on a finite lattice. *Phys. Rev. B* **11**, 1165–1168.

Swendsen, R. H. and Zia, R. K. P., 1979, The surprising effectiveness of the Migdal–Kadanoff renormalization scheme. *Phys. Lett.* **69A**, 382–384.

Tjon, J. A., 1974, Numerical study of the renormalization group equations in the four-cell approximations. *Phys. Lett.* **49A**, 289–290.

Tompa, H., 1953, Quasichemical treatment of mixtures of oriented molecules. *J. chem. Phys.* **21**, 250–258.

Vinogradov, S. N. and Linnell, R. H., 1971, *Hydrogen Bonding*. Van Nostrand Reinhold, New York.
Walas, S. M., 1985, *Phase Equilibrium in Chemical Engineering*. Butterworth, Boston.
Walker, J. S., 1982, Exact preservation of the free energy in a modified Migdal–Kadanoff approximation. *Phys. Rev. B* **26**, 3792–3796.
Walker, J. S. and Vause, C. A., 1980, Theory of closed-loop phase diagrams in binary fluid mixtures. *Phys. Lett.* **79A**, 421–424.
Walker, J. S. and Vause, C. A., 1983, Lattice theory of binary fluid mixtures. *J. chem. Phys.* **79**, 2660–2676.
Wheeler, J. C., 1975, Exactly soluble two-component lattice solutions with upper and lower critical solution temperatures. *J. chem. Phys.* **62**, 433–439.
Wheeler, J. C. and Andersen, G. R., 1980, Some interesting new phase diagrams in hydrogen bonded liquid mixtures. *J. chem. Phys.* **73**, 5778–5785.
Widom, B., 1965, Equation of state in the neighborhood of the critical point. *J. chem. Phys.* **43**, 3898–3905.
Wilson, G. M., 1964, A new expression for the excess free energy of mixtures. *J. Am. chem. Soc.* **86**, 127–130.
Wilson, K. G., 1975, Renormalization group: critical phenomena and the Kondo problem, *Rev. mod. Phys.* **47**, 773–840.
Wilson, K. G., 1979, Problems in physics with many scales of length. *Scient. Am.* August, 158–179.
Wilson, K. G., 1983, Renormalization group and critical phenomena. *Rev. mod. Phys.* **55**, 583–600.
Wilson, K. G. and Kogut J., 1974, The renormalization group and the $\varepsilon$ expansion. *Phys. Rep.* **12**, 75–200.

## APPENDIX A. DERIVATIVES OF THE PARTITION FUNCTION

Equations (20)–(22) and (25) are the recursion formulas for the independent parameters and the partition function. Symbolically, the renormalization flow to some fixed point can be represented by

$$\omega \to \omega' \to \ldots \to \omega^{(\infty)}$$
$$\Delta\tilde{\mu} \to \Delta\tilde{\mu}' \to \ldots \to \Delta\tilde{\mu}^{(\infty)}$$

and also

$$g \to g' \to \ldots \to g^{(\infty)}$$
$$Z \to Z' \to \ldots \to Z^{(\infty)}.$$

It is likewise possible to write renormalization equations for $x_A$ and $\langle N_{AB}\rangle$. (In the following the $\langle\ \rangle$ notation is dropped for convenience, that is, it is to be understood that $N_{AB}$ represents the ensemble average $\langle N_{AB}\rangle$.) Equations (13) and (25) and the chain rule for differentiation give

$$(2x_A - 1) = \frac{\partial}{\partial\Delta\tilde{\mu}}\left[\frac{1}{2}\ln 2 + \frac{3}{8}g' + \frac{1}{8}\left(\frac{1}{N'}\ln Z'\right)\right]$$
$$= \frac{3}{8}\left(\frac{\partial g'}{\partial\Delta\tilde{\mu}}\right)_{\omega} + \frac{1}{8}\left(\frac{\partial\Delta\tilde{\mu}'}{\partial\Delta\tilde{\mu}}\right)_{\omega}\frac{\partial}{\partial\Delta\tilde{\mu}'}\left(\frac{1}{N'}\ln Z'\right)$$
$$+ \frac{1}{8}\left(\frac{\partial\omega'}{\partial\Delta\tilde{\mu}}\right)_{\omega}\frac{\partial}{\partial\omega'}\left(\frac{1}{N'}\ln Z'\right)$$

which can be rewritten as

$$(2x_A - 1) = \frac{3}{8}\left(\frac{\partial g'}{\partial\Delta\tilde{\mu}}\right)_{\omega} + \frac{1}{8}(2x_A - 1)'\left(\frac{\partial\Delta\tilde{\mu}'}{\partial\Delta\tilde{\mu}}\right)_{\omega}$$
$$+ \frac{1}{8}\left(\frac{N_{AB}}{N}\right)'\left(\frac{\partial\omega'}{\partial\Delta\tilde{\mu}}\right)_{\omega}. \qquad (A1)$$

The partial derivatives in eq. (A1) can be evaluated by differentiating the recursion relations for the parameters in the Hamiltonian [eqs (20)–(22)]. Note that in writing eq. (A1) use was made of the "primed" analogues of eqs (13) and (14):

$$(2x_A - 1)' = \frac{1}{N'}\left(\frac{\partial\ln Z'}{\partial\Delta\tilde{\mu}}\right)_{\omega'}$$
$$\left(\frac{N_{AB}}{N}\right)' = \frac{1}{N'}\left(\frac{\partial\ln Z'}{\partial\omega'}\right)_{\Delta\tilde{\mu}'}.$$

The analogous recursion relation for $N'_{AB}$ is

$$\frac{N_{AB}}{N} = \frac{3}{8}\left(\frac{\partial g'}{\partial\omega}\right)_{\Delta\tilde{\mu}} + \frac{1}{8}(2x_A - 1)'\left(\frac{\partial\Delta\tilde{\mu}'}{\partial\omega}\right)_{\Delta\tilde{\mu}}$$
$$+ \frac{1}{8}\left(\frac{N_{AB}}{N}\right)'\left(\frac{\partial\omega'}{\partial\omega}\right)_{\Delta\tilde{\mu}} \qquad (A2)$$

Clearly, eqs (A1) and (A2) are two coupled recursion relations that give $x_A$ and $N_{AB}$ in terms of $x'_A$ and $N'_{AB}$. It is convenient to rewrite these linear equations in the following matrix form where $n$ is the number of transformations performed:

$$\begin{bmatrix} 2x_A - 1 \\ N_{AB}/N \end{bmatrix}^{(n)} = \mathbf{A}^{(n)}\begin{bmatrix} 2x_A - 1 \\ N_{AB}/N \end{bmatrix}^{(n+1)} + \underline{B}^{(n)}. \qquad (A3)$$

Here $\mathbf{A}^{(n)}$ and $\underline{B}^{(n)}$ are given by

$$\mathbf{A}^{(n)} = \frac{1}{8}\begin{bmatrix} \left(\frac{\partial\Delta\tilde{\mu}'}{\partial\Delta\tilde{\mu}}\right)_{\omega} & \left(\frac{\partial\omega'}{\partial\Delta\tilde{\mu}}\right)_{\omega} \\ \left(\frac{\partial\Delta\tilde{\mu}'}{\partial\omega}\right)_{\Delta\tilde{\mu}} & \left(\frac{\partial\omega'}{\partial\omega}\right)_{\Delta\tilde{\mu}} \end{bmatrix}$$

$$\underline{B}^{(n)} = \frac{3}{8}\begin{bmatrix} \left(\frac{\partial g'}{\partial\Delta\tilde{\mu}}\right)_{\omega} \\ \left(\frac{\partial g'}{\partial\omega}\right)_{\Delta\tilde{\mu}} \end{bmatrix}$$

where the partial derivatives are evaluated at $(\omega, \Delta\tilde{\mu})^{(n)}$. The repeated application of eq. (A3) yields

$$\begin{bmatrix} 2x_A - 1 \\ N_{AB}/N \end{bmatrix} = \mathbf{A}\left(\mathbf{A}'\begin{bmatrix} 2x_A - 1 \\ N_{AB}/N \end{bmatrix}'' + \underline{B}'\right) + \underline{B}$$
$$\vdots$$
$$= \left[\prod_{n=0}^{x}\mathbf{A}^{(n)}\right]\begin{pmatrix} 2x_A - 1 \\ N_{AB}/N \end{pmatrix}^{(x)} + \sum_{n=0}^{x}\left[\prod_{m=0}^{n}\mathbf{A}^{(m)}\right]\underline{B}^{(n+1)} + \underline{B}. \qquad (A4)$$

Since $\mathbf{A}^{(n)}$ and $\underline{B}^{(n)}$ can be calculated at each iteration, eq. (A4) can be solved for $x_A$ and $N_{AB}$ if the limiting values $(2x_A - 1)^{(\infty)}$ and $(N_{AB}/N)^{(\infty)}$ are known. In practice, it is found that all initial points flow to one of a small number of fixed points (or sinks). These can be tabulated and the limiting thermodynamic properties determined by solving eq. (A3) at the fixed point

$$\begin{pmatrix} 2x_A - 1 \\ N_{AB}/N \end{pmatrix}^{(x)} = \mathbf{A}^{(x)}\begin{pmatrix} 2x_A - 1 \\ N_{AB}/N \end{pmatrix}^{(x)} + \underline{B}^{(x)} \qquad (A5)$$

where $(\infty)$ denotes values at the fixed point. These values are then used in eq. (A4) to determine the thermodynamic properties at states other than the fixed point.

## APPENDIX B. CRITICAL EXPONENTS

It is possible to show that there is a direct relationship between the recursion relations linearized at a fixed point and

the critical exponents characteristic of that fixed point (Niemeijer and Leeuwen, 1976). Consider the zero field case of the simple Ising model—$\Delta\tilde{\mu} = 0$. From eqs (20) and (21), it is clear that $\Delta\tilde{\mu}'$ is also equal to zero, that is, $\Delta\tilde{\mu} = 0$ defines an invariant-subspace of the phase space under the MK renormalization transformation for the simple Ising model. Thus, the recursion relations can be represented formally as

$$\omega' = \omega'(\omega).$$

Suppose that $\omega^*$ is a fixed point of this recursion relation. Then the transformation can be linearized about $\omega^*$:

$$\omega' - \omega^* + \left(\frac{\partial\omega'}{\partial\omega}\right)_{\omega^*}(\omega - \omega^*) + \ldots \qquad \text{(B1)}$$

[If there are many parameters in the Hamiltonian, and if it lacks the symmetry of the Ising model, then the full recursion relations will have to be linearized, and the partial derivative in eq. (B1) will be replaced by a matrix of derivatives, $\mathbf{D}^*$.] It is clear from eq. (25) that the configurational partition function is related to the renormalized partition function by an expression of the form

$$z(\omega) = g(\omega) + b^{-d}z(\omega')$$

where $z \equiv Z/N$, not to be confused with the lattice coordination number, is proportional to the thermodynamic potential per particle, $b$ is the factor by which the lattice is rescaled ($b = 2$ in the example of Section 6), $d$ is the dimensionality ($d = 3$ for fluid mixture models), and $g(\omega)$ is some non-singular (analytic) function of $\omega$. Near the fixed point this equation can be rewritten in terms of deviation variables as

$$\begin{aligned} z(\omega - \omega^*) &= g(\omega - \omega^*) + b^{-d}z(\omega' - \omega^*) \\ &= g(\omega - \omega^*) + b^{-d}z[\lambda(\omega - \omega^*)] \end{aligned} \qquad \text{(B2)}$$

where $\lambda$ is the partial derivative in eq. (B1). (If there is more than one parameter in the Hamiltonian then $\underline{\lambda}$ is the vector of eigenvalues of the matrix $\mathbf{D}^*$.) Suppose that the thermodynamic potential has a singular power-law dependence on $(\omega - \omega^*)$ at the fixed point, that is

$$z(\omega - \omega^*) = a \times (\omega - \omega^*)^\alpha \qquad \text{(B3)}$$

where $a$ and $\alpha$ are constants that characterize the singular behavior—$\alpha$ is a critical exponent. Then, substituting eq. (B3) into eq. (B2) gives

$$a(\omega - \omega^*)^\alpha = b^{-d}a\lambda^\alpha(\omega - \omega^*)^\alpha.$$

Notice that $g$ does not appear since it was assumed to be non-singular. Solving for $\alpha$ gives

$$\alpha = \mathrm{d}\frac{\ln b}{\ln \lambda}.$$

Thus, if singular behavior occurs, the critical exponent characterizing the divergence depends only on the linearized recursion relation (or on its eigenvalues if there are several parameters), on the scaling factor, and on the dimensionality. The reader is referred to the Niemeijer and Leeuwen (1976) for details on how specific critical exponents, characterizing, for example, the curvature of the coexistence curve at a consolute point, are related to the individual eigenvalues of the linearized transformation.